Inorganic Chemistry

Article

pubs.acs.org/IC

# Flexible Coordination of Diphosphine Ligands Leading to cis and trans Pd(0), Pd(II), and Rh(I) Complexes

Cezar C. Comanescu and Vlad M. Iluc*

Department of Chemistry and Biochemistry, University of Notre Dame, Notre Dame, Indiana 46556, United States

Supporting Information

**ABSTRACT:** A series of diphosphine ligands $^{i}Pr_2P-C_6H_4-X-C_6H_4-P^{i}Pr_2$ (for ligand $L^1$, X = $CH_2$; for ligand $L^2$, X = $CH_2CH_2$) was investigated to determine the preference for cis/trans coordination to palladium(0), palladium(II), and rhodium(I). Increasing the length of the bridging alkyl backbone from one to two carbons changes the geometry of the resulting palladium(II) complexes, with $L^1$ coordinating preferentially cis, while $L^2$ coordinates in a trans fashion. Coordination to Pd(0) leads to $L^1$Pd(dba) and $L^2$Pd(dba), in which both ligands accommodate a P−M−P angle close to 120°. $L^2$ was found to coordinate cis in a rhodium(I) complex ($[L^2Rh(nbd)][BF_4]$, where nbd = norbornadiene).

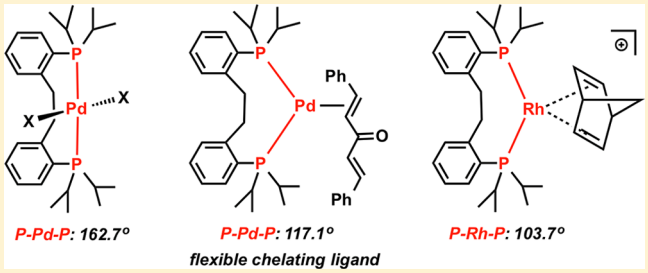


## INTRODUCTION

Diphosphine ligands have played an important role in organometallic chemistry, especially because of their ability to support metal complexes that are highly active in catalysis.[1] Most bidentate ligands have a strong preference toward cis coordination,[2−6] although examples of trans-chelating ligands are known.[7−21] While cis-chelating diphosphines, with bite angles of ∼90°, have been employed for many decades,[22] the first ligand designed to coordinate trans to a metal center dates from 1976. Known as TRANSPHOS, it is still arguably the diphosphine that received the most attention among trans-spanning ligands.[23] Although it strongly prefers a trans coordination, when it shows bite angles ranging from 168° to 176°, some examples of tetracoordinate and tricoordinate complexes with smaller bite angles (ca. 105°) have been reported.[24] Cis coordination of TRANSPHOS is typically accompanied by bending of the phenanthrene backbone, while the methylene groups increase the ligand's flexibility (see Figure 1). As pointed out in a recent review, only a few diphosphines are known to coordinate in a trans fashion with a P−M−P angle close to 180°.[7]

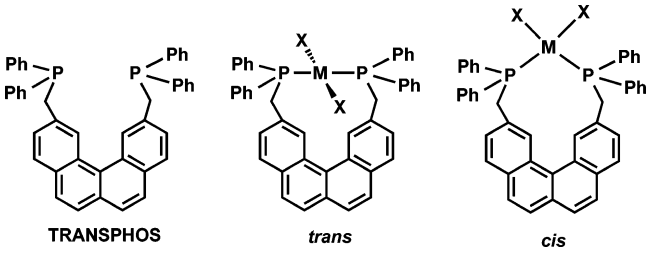


**Figure 1.** TRANSPHOS and its two coordination modes.

The factors determining the coordination mode of certain diphosphines are still intensely studied since they can bind either cis or trans, depending on the reaction conditions.[13,15−17] Although known for some time, ancillary ligand flexibility features prominently in recent studies with some examples, in which the ligand actively participates in the reactions of the metal, known as metal−ligand cooperation.[25−30] We became interested in studying flexible ligand backbones[31−39] and decided to determine whether we can control the cis or trans coordination preference of certain diphosphines. Therefore, we synthesized the diphosphines $^{i}Pr_2P-C_6H_4-X-C_6H_4-P^{i}Pr_2$ (for ligand $L^1$, X = $CH_2$; for ligand $L^2$, X = $CH_2CH_2$) derived from modified pincer backbones that show cis and trans coordination to different metal centers. In addition, the resulting Pd(II) complexes behave as active catalysts in Suzuki and Heck coupling reactions.

## RESULTS AND DISCUSSION

**Synthesis and Structural Characterization of Metal Complexes.** Recently, Piers and Parvez reported a new diphosphine with a modified pincer backbone, $^{i}Pr_2P(o\text{-}C_6H_4-CH_2-o'\text{-}C_6H_4)P^{i}Pr_2$ ($L^1$).[40−42] When employed in conjunction with iridium, a double C−H activation leading to an Ir carbene was observed.[43] This ligand design was inspired by the pioneering work of Floriani et al., who synthesized the phenyl derivative and explored its reactivity with Ni, Pd, Pt, Fe, and Rh precursors.[44] We postulated that increasing the length of the backbone might force the ligand to coordinate preferentially in a trans fashion.

The diphosphine syntheses are straightforward[43] and afford products in high yields. Compound $^{i}Pr_2P(o\text{-}C_6H_4-CH_2CH_2-$

Received: May 9, 2014
Published: August 7, 2014

   dx.doi.org/10.1021/ic5010566 | Inorg. Chem. 2014, 53, 8517−8528

**Scheme 1. Syntheses of Palladium Complexes**

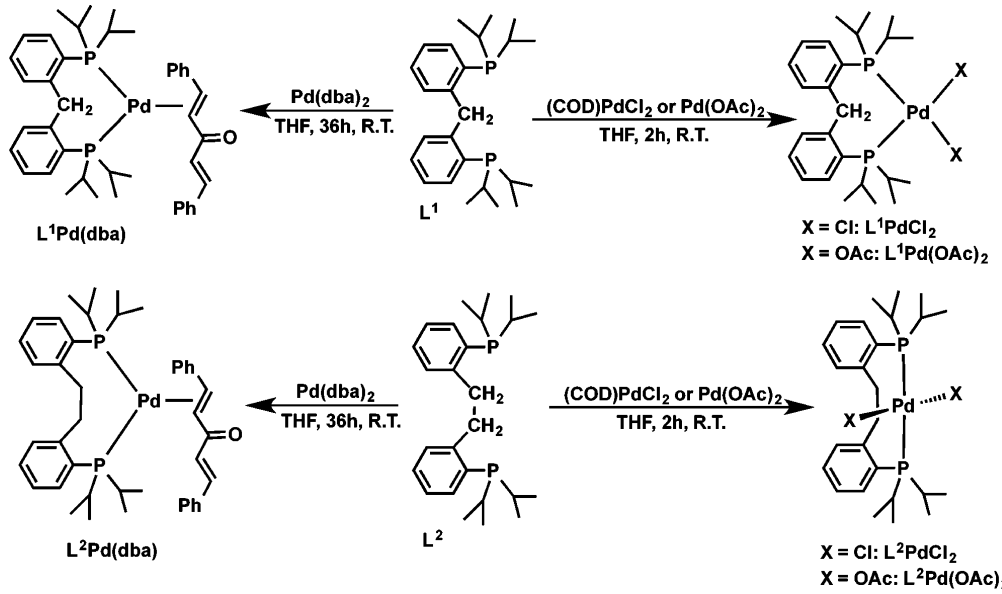


$o'$-$C_6H_4$)P$^i$Pr$_2$ ($L^2$) was synthesized from 2-bromomethylbromobenzene,[45,46] in 91% yield. $L^2$ was structurally characterized in the solid state by single-crystal X-ray diffraction (see Figure SX24 in the Supporting Information).

The reaction between $L^1$ or $L^2$ and Pd(COD)Cl$_2$ in THF at room temperature for 2 h (Scheme 1) led to the precipitation of L$^i$PdCl$_2$ ($i$ = 1 or 2), yellow compounds, which were isolated in high yield. Analogously, the reaction between L$^i$ and Pd(OAc)$_2$ in THF at room temperature for 2 h led to the isolation of the corresponding palladium(II) acetate complexes, L$^i$Pd(OAc)$_2$ in high yield (Scheme 1). All four metal complexes were characterized by single-crystal X-ray diffraction (Figures 2–5). As expected, the two $L^1$ complexes, $L^1$PdCl$_2$ (Figure 2) and $L^1$Pd(OAc)$_2$ (Figure 3), show cis coordination of the diphosphine. The coordination of the diphosphine to the Pd(II) center is accompanied by a downfield shift in the $^{31}$P NMR spectrum from −5.87 ppm (in $L^1$) to 38.47 ppm (broad, $CD_2Cl_2$) for $L^1$PdCl$_2$ and to 34.62 ppm in the case of $L^1$Pd(OAc)$_2$. The solid-state molecular structures of $L^1$PdCl$_2$ and $L^1$Pd(OAc)$_2$ show a square-planar geometry at Pd(II) with the sum of angles around the metal center of ca. 360° (360.38° for $L^1$PdCl$_2$ and 360.90° for $L^1$Pd(OAc)$_2$). The P(1)–Pd–P(2) angles are 100.02(5)° in $L^1$PdCl$_2$ and 101.06(3)° in $L^1$Pd(OAc)$_2$, which is consistent with the cis coordination mode of $L^1$.

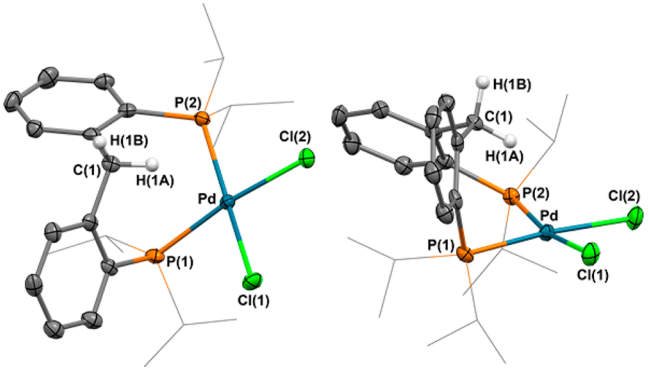


**Figure 2.** (Left) Molecular structure of $L^1$PdCl$_2$ with thermal ellipsoids at 50% probability. (Right) View showing the anagostic interaction between H(1A)–Pd. All hydrogen atoms except those involved in the anagostic interaction were omitted for clarity. Selected bond distances: Pd–Cl(1) = 2.3765(13) Å, Pd–Cl(2) = 2.3559(13) Å, Pd–P(1) = 2.3311(13) Å, Pd–P(2) = 2.2742(13) Å, Pd–H(1A) = 2.393 Å, Pd–H(1B) = 4.014 Å. Selected bond angles: P(1)–Pd–Cl(1) = 84.87(5)°, Cl(1)–Pd–Cl(2) = 88.40(5)°, Cl(2)–Pd–P(2) = 87.09(5)°, P(2)–Pd–P(1) = 100.02(5)°, Pd–H(1A)–C(1) = 140.76°.

On the other hand, $L^2$ coordinates in a trans fashion to palladium(II), leading to $L^2$PdCl$_2$ (Figure 4) and $L^2$Pd(OAc)$_2$ (Figure 5). A slight increase of the P–Pd–P angle, from 162.72(2)° in $L^2$PdCl$_2$ to 163.31(6)° in $L^2$Pd(OAc)$_2$, was observed, which was likely a consequence of the additional steric bulk of the acetate ligands. The sum of angles around Pd(II) is close to 360° in both complexes (361.54° for $L^2$PdCl$_2$ and 358.94° for $L^2$Pd(OAc)$_2$), as expected for a square planar geometry at the metal center (Figures 4 and 5).

In order to determine the influence of the metal oxidation state on the resulting geometry, reactions between the two diphosphines and Pd(dba)$_2$ were carried out (Scheme 1). Although the two diphosphines showed different coordination modes with palladium(II), they both behave as wide-angle ligands when coordinated to the Pd(dba) moiety, a coordination mode enforced by the oxidation state of palladium. The P–Pd–P angle is 113.33(5)° in $L^1$Pd(dba) and 117.117(17)° in $L^2$Pd(dba). Both L$^i$Pd(dba) complexes (Figures 6 and 7) have the sum of angles around the metal center close to 360°, as expected for a trigonal planar geometry at palladium (if dba is considered to occupy only one coordination site).

In order to determine whether $L^2$ can adapt its coordination in response to the presence of a cis enforcing ligand, the reaction between $L^2$ and [Rh(nbd)$_2$][BF$_4$] (where nbd = 1,5-norbornadiene) was carried out and led to [$L^2$Rh(nbd)][BF$_4$] (eq 1). Its solid-state molecular structure (Figure 8) was determined by single crystal X-ray diffraction, which indicated that the P–Rh–P angle is 103.74(2)°. A search in the Cambridge Structural Database showed that this value is the second largest in [Rh(P–P)(nbd)]$^+$ complexes (77 examples).


dx.doi.org/10.1021/ic5010566 | Inorg. Chem. 2014, 53, 8517–8528

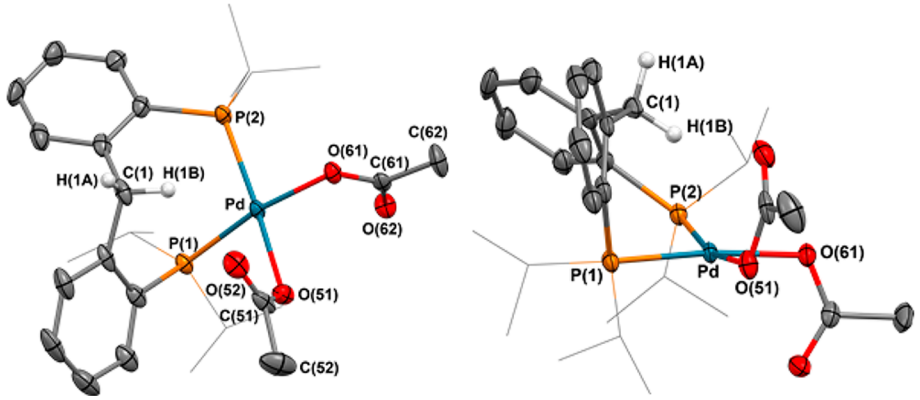


**Figure 3.** (Left) Molecular structure of $L^1Pd(OAc)_2$ with thermal ellipsoids at 50% probability. (Right) View showing the anagostic interaction between H(1B)−Pd. Co-crystallized solvent molecules and all hydrogen atoms except those involved in the anagostic interaction were omitted for clarity. Selected bond distances: P(1)−Pd = 2.2759(7) Å, Pd−O(51) = 2.0981(19) Å, Pd−O(61) = 2.0871(18) Å, Pd−P(2) = 2.2486(8) Å, Pd−H(1B) = 2.615 Å, Pd−H(1A) = 4.070 Å. Selected bond angles: P(1)−Pd−O(51) = 83.67(6)°, O(51)−Pd−O(61) = 88.42(7)°, O(61)−Pd−P(2) = 87.75(6)°, P(2)−Pd−P(1) = 101.06(3)°, Pd−H(1A)−C(1) = 139.93°.

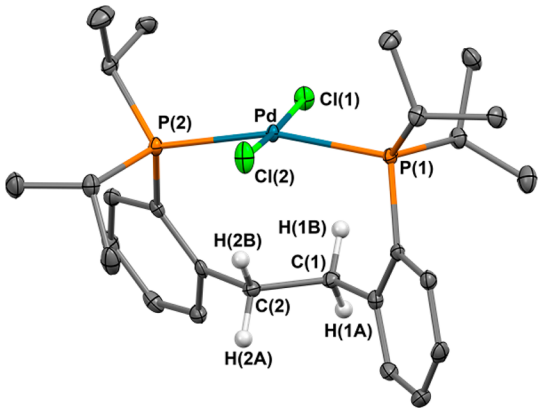


**Figure 4.** Molecular structure of $L^2PdCl_2$ with thermal ellipsoids at 50% probability showing the anagostic interaction H(1B)−Pd and H(2B)-Pd. All hydrogen atoms except those involved in the anagostic interaction were omitted for clarity. Selected bond distances: Pd−Cl(1) = 2.3146(6) Å, Pd−Cl(2) = 2.3049(6) Å, Pd−P(1) = 2.3372(6) Å, Pd−P(2) = 2.3483(6) Å, Pd−H(1A) = 4.169 Å, Pd−H(1B) = 2.788 Å, Pd−H(2A) = 3.979 Å, Pd−H(2B) = 2.523 Å. Selected bond angles: P(2)−Pd−Cl(1) = 88.75(2)°, Cl(1)−Pd−P(1) = 92.67(2)°, P(2)−Pd−Cl(2) = 93.47(2)°, Cl(2)−Pd−P(1) = 86.65(2)°, P(1)−Pd−P(2) = 162.72(2)°, Pd−H(1B)−C(1) = 113.63°, Pd−H(2B)−C(2) = 124.41°.

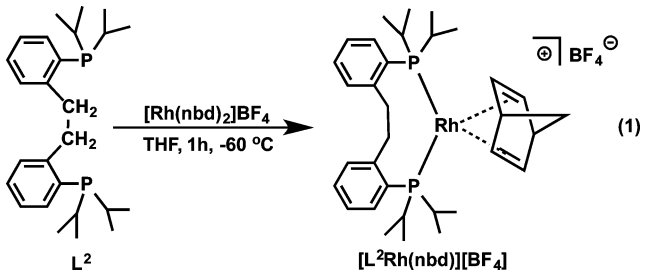


These angles range from 73.69° in [Rh(2-phosphino-2,3-dihydrobenzo-[d][1,3]oxaphosphole)(nbd)][$BF_4$][47] to 104.52° in [($^{iPr}$DPDBFphos)Rh(nbd)][$BF_4$].[17] The value of the P−metal−P angle changed by ca. 15° from $L^2Pd(dba)$ to [$L^2$Rh(nbd)][$BF_4$]. The $^{31}P-^{103}Rh$ coupling constant of 119.6 Hz is in agreement with previously reported values for wide-angle diphosphine ligands.[7]

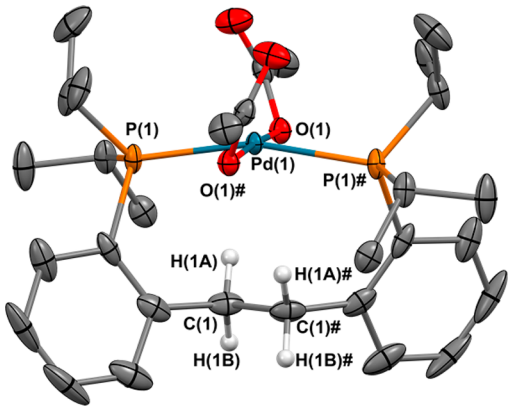


**Figure 5.** Molecular structure of $L^2Pd(OAc)_2$ with thermal ellipsoids at 50% probability showing the anagostic interaction H(1A)−Pd. Co-crystallized solvent molecules and all hydrogen atoms except those involved in the anagostic interaction were omitted for clarity. Selected bond angles: Pd(1)−O(1) = 2.032(2) Å, Pd(1)−P(1) = 2.3575(10) Å, Pd1−H(1A) = 2.599 Å, Pd(1)−H(1B) = 4.091 Å. Selected bond distances: O(1)−Pd(1)−P(1) = 89.10(7)°, P(1)−Pd(1)−O(1)# = 90.37(7)°, P(1)−Pd(1)−P(1)# = 163.31(6)°, Pd(1)−H(1A)−C(1) = 117.87°.

We became interested to determine the geometry of palladium(0) complexes in the absence of dba. Reactions of $L^iPdCl_2$ ($i$ = 1, 2) with either Mg/THF at room temperature overnight or with $LiBEt_3H$ for 4 h led to palladium(0) complexes (Scheme 2). The same product was obtained independently of the reduction method used, as confirmed by $^1H$, $^{31}P$, and $^{13}C$ NMR spectroscopy. X-ray crystallography established that reduction of $L^2PdCl_2$ yields a monomeric complex, $L^2Pd$ (Figure 9). Because $L^1$ cannot accommodate a trans-spanning geometry, a dimeric palladium(0) complex, $[L^1Pd]_2$, was formed (Figure 10). The P−Pd−P angles are 167.87(9)°, 170.82(9)°, 166.68(9)°, and 172.81(9)° for the two similar units in $[L^1Pd]_2$, while in the monomeric $L^2Pd$, the corresponding P−Pd−P angle is 163.38(2)°.

**Anagostic Interactions.** All palladium complexes described above exhibit anagostic interactions. Anagostic interactions[48] refer to any M−H−C interactions that are not agostic[49,50] and are special cases of hydrogen bonding. The metal complexes featuring such interactions have a relatively


dx.doi.org/10.1021/ic5010566 | Inorg. Chem. 2014, 53, 8517−8528

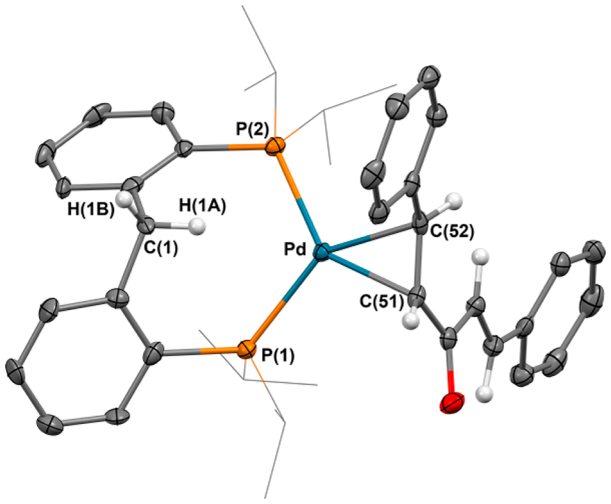


**Figure 6.** Molecular structure of $L^1Pd(dba)$ with thermal ellipsoids at 50% probability. Most hydrogen atoms were omitted for clarity. Selected bond distances: Pd–P(1) = 2.3953(13) Å, Pd–P(2) = 2.3337(13) Å, Pd–C(51) = 2.155(4) Å; Pd–C(52) = 2.144(4) Å. Selected bond angles: P(1)–Pd–P(2) = 113.33(5)°, P(1)–Pd–C(51) = 104.70(12)°, C(51)–Pd–C(52) = 38.74(16)°, C(52)–Pd–P(2) = 103.68(13)°.

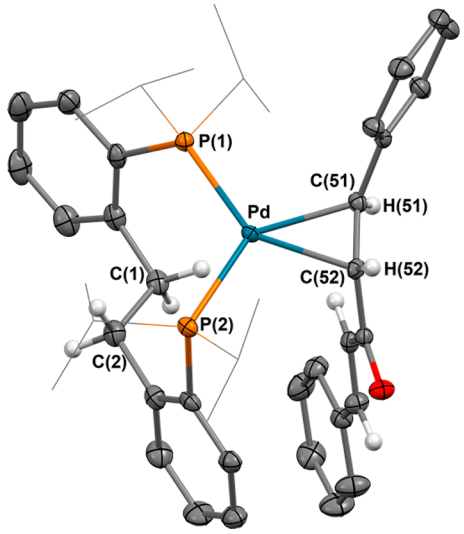


**Figure 7.** Molecular structure of $L^2Pd(dba)$ with thermal ellipsoids at 50% probability. Most hydrogen atoms were omitted for clarity. Selected bond distances: Pd–P(1) = 2.3390(5) Å, Pd–P(2) = 2.3473(5) Å, Pd–C(51) = 2.1432(18) Å, Pd–C(52) = 2.1333(15) Å. Selected bond angles: P(1)–Pd–P(2) = 117.117(17)°, P(2)–Pd–C(52) = 100.28(7)°, P(2)–Pd–C(51) = 139.15(5)°, C(51)–Pd–C(52) = 38.88(8)°, C(51)–Pd–P(1) = 103.73(5)°.

long M–H distance (2.3–2.9 Å), a large M–H–C angle (110–170°), and show an unusual shift of several ppm downfield from the uncoordinated CH of the ligand precursor in their $^1H$ NMR spectra.[51−53] Anagostic interactions are usually associated with $d^8$ metal centers, which are square planar prior to the interaction, and are critically dependent on the metal center, as Bergman and co-workers showed in their investigations on Rh(I) complexes.[51,54] Bergman's group conducted a theoretical study to elucidate the origin of the anagostic interaction and found that it can vary from purely electrostatic (hydrogen bonding, extreme case) to an electrostatic–partially covalent interaction (stronger interaction, shorter M–H distances).[51]

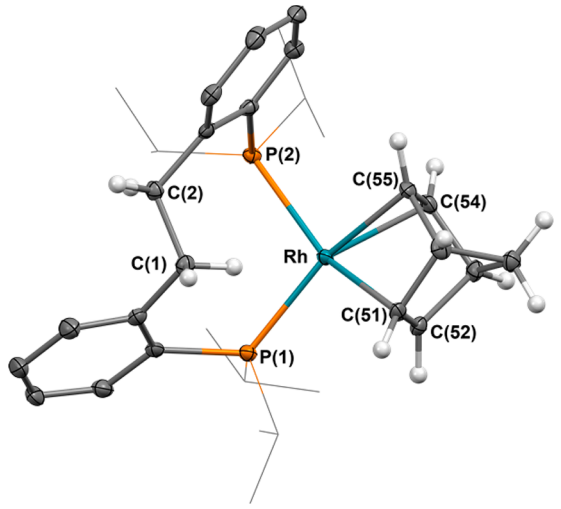


**Figure 8.** Molecular structure of $[L^2Rh(nbd)][BF_4]$ with thermal ellipsoids at 50% probability. Most hydrogen atoms and the counterion were omitted for clarity. Selected bond distances: Rh–C(51) = 2.169(2) Å, Rh–C(52) = 2.191(2) Å, Rh–C(54) = 2.225(2) Å, Rh–C(55) = 2.206(2) Å, Rh–P(1) = 2.3548(6) Å, Rh–P(2) = 2.4349(6) Å. Selected bond angle: P(1)–Rh–P(2) = 103.74(2)°.

**Scheme 2. Reduction of $L^iPdCl_2$ ($i$ = 1, 2)**

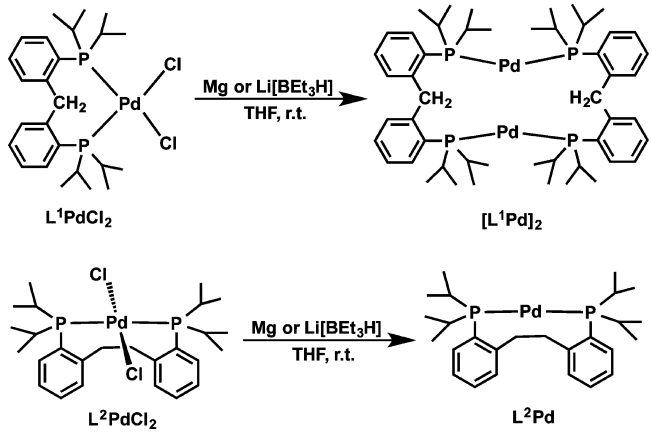


The effect of the anagostic interaction is dependent on the X ligand coordinated to the metal center of interest, as the $CH_3COO^-$ group induces a larger splitting of the chemical shifts for the two protons than $Cl^-$, and also on the solvent used (different shifts are recorded for the $H_{endo}$ and $H_{exo}$ in $L^1Pd(OAc)_2$ in $CD_2Cl_2$ versus $C_6D_6$). As a consequence, in $L^1Pd(OAc)_2$, the exoproton has a chemical shift at 3.88 ppm as a doublet due to H–H coupling ($J_{HH}$ = 20 Hz), while the endohydrogen is shifted to 8.05 ppm (dt, $J_{HH}$ = 20 Hz, $J_{HP}$ = 2.86 Hz; see Figure 11).

The backbone methylene protons of $L^1$ appear as a triplet in its $^1H$ NMR spectrum at 5.16 ppm, due to their coupling with the two equivalent $^{31}P$ nuclei ($J_{HP}$ = 4.05 Hz). Upon coordination to palladium(II) (in $L^1PdCl_2$ and $L^1Pd(OAc)_2$), the two protons are not equivalent anymore and their chemical shift is significantly different (see Table 1): the exoproton, which is further away from palladium, shows a relatively close chemical shift to that of the corresponding proton in the free ligand: 4.07 ppm (d, $J_{H-H}$ = 11.9 Hz) in $L^1PdCl_2$, while the endoproton, because of its interaction with palladium, shows a


dx.doi.org/10.1021/ic5010566 | Inorg. Chem. 2014, 53, 8517–8528

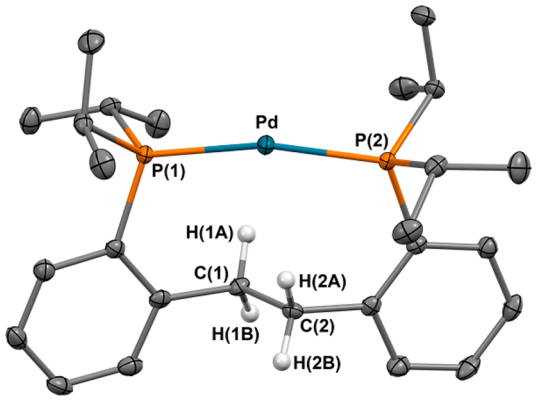


**Figure 9.** Molecular structure of $L^2Pd$ with thermal ellipsoids at 50% probability showing the anagostic interactions H(1A)−Pd and H(2A)−Pd. All hydrogen atoms except those involved in the anagostic interaction were omitted for clarity. Selected bond distances: Pd−P(1) = 2.2659(7) Å, Pd−P(2) = 2.2623(7) Å, Pd−H(1A) = 2.59 Å, Pd−H(1B) = 3.97 Å, Pd−H(2A) = 2.62 Å, Pd−H(2B) = 3.98 Å. Selected bond angles: P(1)−Pd−P(2) = 163.38(2)°, Pd−H(1A)−C(1) = 120.53°, Pd−H(2A)−C(2) = 122.60°.

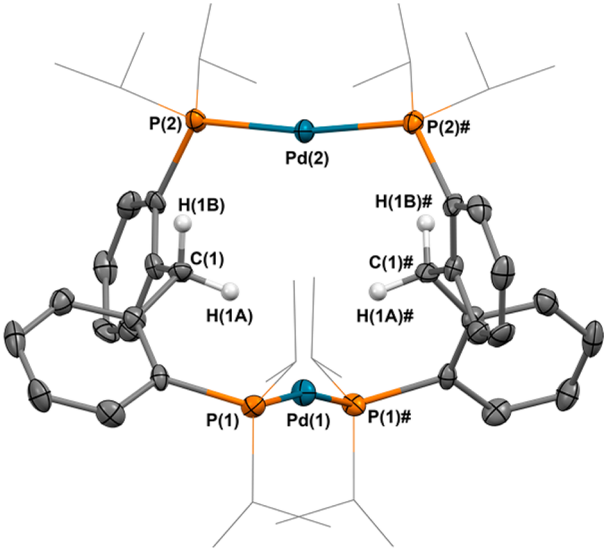


**Figure 10.** Molecular structure of $[L^1Pd]_2$ with thermal ellipsoids at 50% probability (only one of the crystallographically independent molecules in the unit cell is shown). Most hydrogen atoms were omitted for clarity. Selected bond distances: Pd(1)−P(1) = 2.2691(15) Å, Pd(2)−P(2) = 2.2710(15) Å. Selected bond angles: P(1)−Pd(1)−P(1)# = 167.87(9)°; P(2)−Pd(2)−P(2)# = 170.82(9)°.

downfield shift at 6.93 ppm (dt, $J_{HH}$ = 11.9 Hz and $J_{HP}$ = 2.1 Hz).

**DFT Calculations.** The ability of $L^2$ to accommodate both cis and trans isomers was investigated using density functional theory (DFT). The intermediate structures were optimized for $L^2PdCl_2$ constraining only the P−Pd−P angle at values between 90 and 180° in 5° increments. Then, a single-point energy was calculated for each conformer of the ligand by removing the $PdCl_2$ group (Figure 12). The difference between the two conformers resulting from the *cis*-$L_2PdCl_2$ and *trans*-$L_2PdCl_2$ isomers is only 12.4 kcal/mol, in agreement with the observed ability of this ligand to adopt both conformations (Figure 12). The energy drops rapidly from 90° (+12.4 kcal/mol) to 120° (+4.8 kcal/mol), the angle usually observed for trigonal planar Pd(0) complexes.

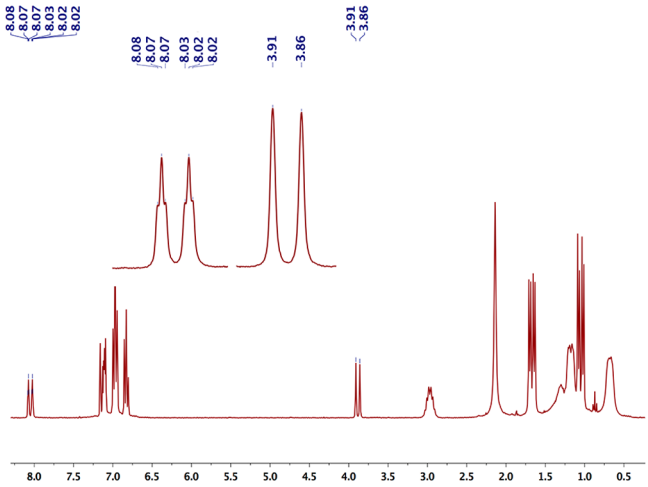


**Figure 11.** $^1H$ NMR ($C_6D_6$) spectrum of $L^1Pd(OAc)_2$ depicting the anagostic interaction in the two insets (downfield, endo proton; upfield, exo proton).

**Table 1. Chemical Shift (ppm) and Distances to Palladium for the Protons Involved in Anagostic Interactions**

| metal complex | endo δ (ppm) | exo δ (ppm) | Pd−H endo (Å) | Pd−H exo (Å) |
|---|---|---|---|---|
| $L^1PdCl_2$ | 6.93 | 4.07 | 2.39 | 4.01 |
| $L^1Pd(OAc)_2$ | 8.05 | 3.88 | 2.59 | 4.09 |
| $L^2PdCl_2$ | 5.15 | 2.97 | 2.52, 2.78 | 3.97, 4.16 |
| $L^2Pd(OAc)_2$ | 5.33 | 3.08 | 2.59 | 4.09 |
| $L^2Pd$ | 5.85 | 2.54 | 2.59, 2.62 | 3.97, 3.98 |
| $L^2Pd(p\text{-}C_6H_4\text{-}NO_2)Br$ | 4.56, 4.11 | 2.90, 2.80 | 2.57, 2.76 | 4.08, 4.21 |

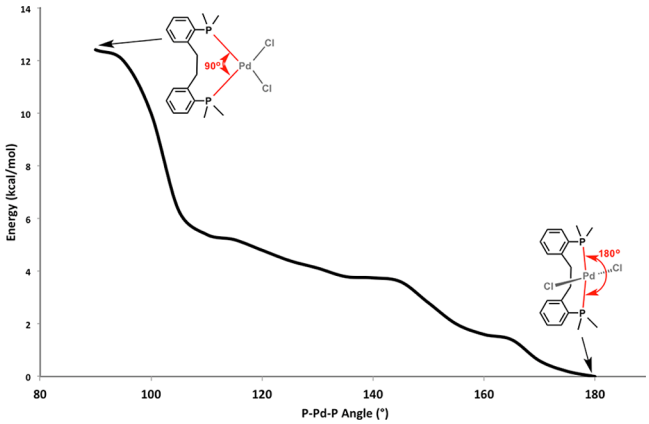


**Figure 12.** Calculated energies for the different conformations of $L^2$ as a ligand for palladium(II).

**C−C Cross-Coupling Reactions.** Palladium complexes supported by bidentate phosphines, including trans-spanning ligands,[3,55] were reported to be active catalysts in C−C cross coupling reactions. In order to determine whether the flexibility of the ligand coordination is important to catalytic activity, the reactivity of $L^1Pd(OAc)_2$, $L^2Pd(OAc)_2$, $L^1PdCl_2$, and $L^2PdCl_2$ was tested in the coupling of aryl halides with phenyl boronic acid (Table 2). Although aryl chlorides are unreactive (see entries 13 and 14 in Table 2), all four palladium complexes catalyzed the coupling of aryl bromides and iodides (see entries


dx.doi.org/10.1021/ic5010566 | Inorg. Chem. 2014, 53, 8517−8528

**Table 2. Suzuki Coupling Reactions Using $L^1PdCl_2$ and $L^2PdCl_2$ as Precatalysts**

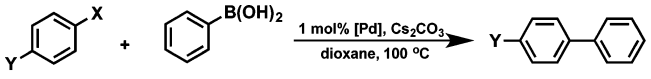


X = I, Br, Cl
Y = $COCH_3$, H, $OCH_3$, $CH_3$

| entry | substrate | precatalyst | time (h) | yield (%) |
|---|---|---|---|---|
| 1 | *p*-Br−$C_6H_4$−$COCH_3$ | $L^1PdCl_2$ | 12 | 84 |
| 2 | *p*-Br−$C_6H_4$−$COCH_3$ | $L^2PdCl_2$ | 12 | 74 |
| 3 | *p*-Br−$C_6H_4$−$NO_2$ | $L^1PdCl_2$ | 6 | 82 |
| 4 | *p*-Br−$C_6H_4$−$NO_2$ | $L^2PdCl_2$ | 6 | 74 |
| 5 | $C_6H_5Br$ | $L^1PdCl_2$ | 3 | 78 |
| 6 | $C_6H_5Br$ | $L^2PdCl_2$ | 3 | 61 |
| 7 | *p*-I−$C_6H_4$−$NO_2$ | $L^1PdCl_2$ | 5 | 91 |
| 8 | *p*-I−$C_6H_4$−$NO_2$ | $L^2PdCl_2$ | 5 | 92 |
| 9 | $C_6H_5I$ | $L^1PdCl_2$ | 3 | 63 |
| 10 | $C_6H_5I$ | $L^2PdCl_2$ | 3 | 56 |
| 11 | *p*-I−$C_6H_4$−$OCH_3$ | $L^1PdCl_2$ | 17 | 77 |
| 12 | *p*-I−$C_6H_4$−$OCH_3$ | $L^2PdCl_2$ | 17 | 62 |
| 13 | *p*-Cl−$C_6H_4$−$CH_3$ | $L^1PdCl_2$ | 8 | 0 |
| 14 | *p*-Cl−$C_6H_4$−$CH_3$ | $L^2PdCl_2$ | 8 | 0 |

1−12 in Table 2). Attempts to use $K_2CO_3$ instead of the stronger base $Cs_2CO_3$ led to lower yields (25%−30% lower, on average). As previously reported,[56−59] catalyst loadings higher than 0.1 mol % led to a lower turnover frequency (TOF), bercause of catalyst deactivation. It is likely that palladium nanoparticles form and agglomerate since the formation of palladium black is observed.

The same four palladium complexes also act as precatalysts in the Heck coupling of aryl halides with *n*-butyl acrylate (Table 3). In addition to the results presented in Table 3, the coupling of 1-hexene with 4-nitro-1-iodobenzene in 3 h (same conditions as above), catalyzed by $L^2PdCl_2$, led to the expected product in 61% yield.

In order to determine whether the reaction proceeds heterogeneously and the homogeneous catalysts lead to the formation of colloidal particles, a mercury test was conducted. Carrying out the Suzuki coupling reaction of phenylboronic acid with *p*-nitrobromobenzene in 1,4-dioxane, using 1% $L^2PdCl_2$ and conditions similar to those previously described led to 61.5% conversion to 4-nitrobiphenyl when one drop of Hg was added to the reaction mixture prior to heating. Although a drop in yield is apparent, the reaction was not shut down, indicating that the likely mechanism of catalysis is homogeneous. These findings agree with the accepted view of a homogeneous mechanism for C−C cross-coupling reactions that is operating even in the case of nanoparticulate palladium.[59−64]

In order to determine whether the phosphines may dissociate during catalysis, the reaction of $L^1PdCl_2$ or $L^2PdCl_2$ with 2 equiv of $BF_3$ at ambient temperature for 3 h in THF was carried out. Although no considerable decomposition was observed, the results are consistent with the possibility that each phosphine may dissociate during catalysis; for instance, $L^1PdCl_2$ is still ∼80% present in the resulting mixture, in the case of $L^2PdCl_2$ treatment with $BF_3$.

In order to probe whether $L^2$ undergoes a trans−cis isomerization during catalysis, the stoichiometric reaction between $L^2Pd$ and *p*-nitrobromobenzene was carried out and led to the formation of *trans*-$L^2Pd(p\text{-}C_6H_4\text{−}NO_2)Br$, in which $L^2$ retains the trans coordination to the palladium center (P−Pd−P angle is 162.84(2)°). (The molecular structure of $L^2Pd(p\text{-}C_6H_4\text{−}NO_2)Br$ is shown in Figure 13.) The oxidative addition to a trans spanning Pd-diphosphine complexes leading also to a trans Pd(II) complex is a rare event and is associated with isomerization. For instance, complexes of the type [(Xantphos)Pd(Aryl)]X (X = halide) show trans coordination, although the ligand itself is known to exhibit both cis and trans coordination.[65−67] Thiel et al. reacted Xantphos with $Pd(dba)_2$ and 4-trifluoromethyl-bromobenzene to obtain *trans*-(Xantphos)Pd(4-trifluoromethylphenyl)(Br), which features a P−Pd−P angle of 153.07(3)°.[68] Similarly, treatment of Xantphos with $Pd_2(dba)_3$ and 4-bromobenzonitrile led to *trans*-(Xantphos)Pd(4-cyanophenyl)Br, which was characterized crystallographically and a large P−Pd−P angle of 150.7° was found by Yin and Buchwald.[66] Van Leeuwen et al.

**Table 3. Heck Coupling Results Using $L^1PdCl_2$ and $L^2PdCl_2$ as Catalysts**

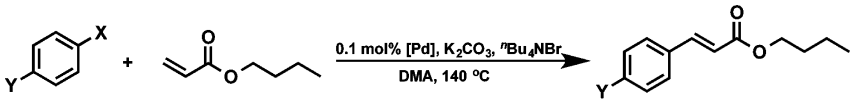


X = I, Br, Cl
Y = $COCH_3$, $NO_2$, H, $OCH_3$, $CH_3$

| entry | substrate | precatalyst | time (h) | yield(%) |
|---|---|---|---|---|
| 1 | *p*-Br−$C_6H_4$−$COCH_3$ | $L^1PdCl_2$ | 4 | 63 |
| 2 | *p*-Br−$C_6H_4$−$COCH_3$ | $L^2PdCl_2$ | 4 | 78 |
| 3 | *p*-Br−$C_6H_4$−$NO_2$ | $L^1PdCl_2$ | 4 | 91 |
| 4 | *p*-Br−$C_6H_4$−$NO_2$ | $L^2PdCl_2$ | 4 | 84 |
| 5 | *p*-Br−$C_6H_4$−$CH_3$ | $L^1PdCl_2$ | 8 | 92 |
| 6 | *p*-Br−$C_6H_4$−$CH_3$ | $L^2PdCl_2$ | 8 | 79 |
| 7 | *p*-I−$C_6H_4$−$NO_2$ | $L^1PdCl_2$ | 3 | 88 |
| 8 | *p*-I−$C_6H_4$−$NO_2$ | $L^2PdCl_2$ | 3 | 92 |
| 9 | *p*-I−$C_6H_4$−$OCH_3$ | $L^1PdCl_2$ | 4 | 97 |
| 10 | *p*-I−$C_6H_4$−$OCH_3$ | $L^2PdCl_2$ | 4 | 91 |
| 11 | *p*-I−$C_6H_4$−$CH_3$ | $L^1PdCl_2$ | 4 | 92 |
| 12 | *p*-I−$C_6H_4$−$CH_3$ | $L^2PdCl_2$ | 4 | 88 |
| 13 | *p*-Br−$C_6H_4$−$OCH_3$ | $L^1PdCl_2$ | 8 | 87 |
| 14 | *p*-Br−$C_6H_4$−$OCH_3$ | $L^2PdCl_2$ | 8 | 73 |


dx.doi.org/10.1021/ic5010566 | Inorg. Chem. 2014, 53, 8517−8528

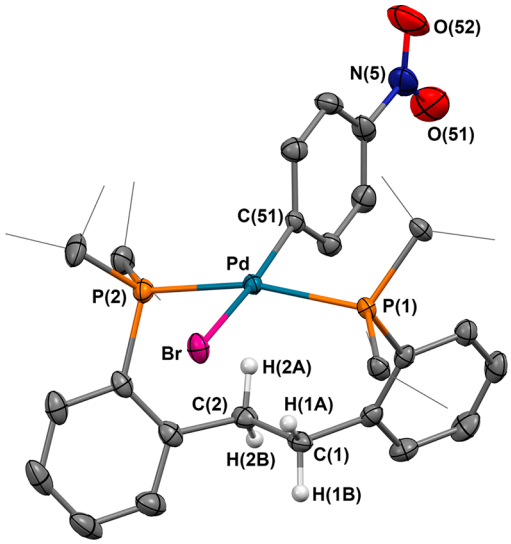


**Figure 13.** Molecular structure of $L^2Pd(p\text{-}C_6H_4{-}NO_2)Br$ with thermal ellipsoids at 50% probability. Most hydrogen atoms were omitted for clarity. Selected bond distances: Pd−P(1) = 2.3331(6) Å, Pd−P(2) = 2.3377(6) Å, Pd−Br = 2.5221(3) Å, Pd−C(51) = 2.021(2) Å, Pd−H(1A) = 2.766 Å, Pd−H(2A) = 2.576 Å. Selected bond angles: P(1)−Pd−P(2) = 162.84(2)°, Br−Pd−C(51) = 172.48(7)°, P(1)−Pd−Br = 94.458(16)°, P(2)−Pd−Br = 86.236(18)°, P(1)−Pd−C(51) = 86.07(7)°, P(2)−Pd−C(51) = 95.48(6)°.

synthesized a series of ligands derived from Xantphos and characterized the neutral complexes (L−L)Pd(4-$C_6H_4CN$)(Br) (L−L is the diphosphine ligand) obtained by reacting the diphosphine with $\{[(o\text{-tolyl})_3P]Pd(4\text{-}C_6H_4CN)Br\}_2$. It was found that the P−Pd−P angles lie in the range of 150.4°−155.0°, confirming the strong preference of the Xantphos motif toward trans coordination.[67] Attempts to monitor the oxidative addition step by NMR spectroscopy did not lead to additional information since the stoichiometric reaction is almost complete by the time an NMR instrument was reached.

Although the flexibility of $L^2$ to adopt various coordination modes may still be important in other reactions, the results of the cross-coupling experiments show that both palladium complexes, $L^1PdCl_2$ and $L^2PdCl_2$, display similar activity. These results are in agreement with the findings from DFT calculations and indicate that the energy necessary to switch between cis and trans coordination modes for $L^2$ is likely smaller than the activation barrier for the turnover-limiting step in these reactions. However, based on results from the reaction of $L^1PdCl_2$ or $L^2PdCl_2$ with 2 equiv of $BF_3$, it is also possible that the phosphine dissociates during catalysis. Since large colloidal particles do not form (Hg test) and the ligands are chelating, it is likely that complete dissociation of the diphosphines does not occur appreciably.

## CONCLUSIONS

New palladium(0) and palladium(II) complexes supported by the bidentate ligands $L^1$ and $L^2$ and a rhodium(I) complex supported by $L^2$ were synthesized and characterized. While $L^1$ has a preference for cis coordination to palladium(II) ($L^1PdCl_2$, $L^1Pd(OAc)_2$), it is flexible enough to adopt a wide angle upon coordination to palladium(0) ($L^1Pd(dba)$), as a response to the geometry enforced by the oxidation state of the metal. In contrast, $L^2$ exhibits a strong preference for trans coordination to palladium(II) and leads to square planar complexes ($L^2PdCl_2$, $L^2Pd(OAc)_2$). However, the same ligand can coordinate as a wide-angle ligand to palladium(0) in order to accommodate a trigonal planar geometry in $L^2Pd(dba)$, in which case the dba molecule plays an important role as a spectator ligand. Comparison of metrical parameters obtained from X-ray crystal structures for palladium complexes (see Table 4) is in agreement with these observations. Aside from the large difference in P−Pd−P angles between cis and trans complexes, palladium(II) complexes supported by $L^1$ show shorter Pd−P distances than the corresponding complexes supported by $L^2$; however, these differences are small. On the other hand, $^{31}P$ NMR chemical shifts are not predictive and do not even differentiate between palladium(0) and palladium(II) complexes. The flexibility of $L^2$ is apparent in its coordination to rhodium(I), when *cis* coordination is observed with a large P−Rh−P angle of 103.75(2)°. In addition, the palladium(II) complexes synthesized herein proved to be active catalysts in Heck and Suzuki C−C couplings, achieving yields in the range of 60%−99%, with the activated aryl iodides giving the fastest and highest conversions among the tested substrates.

**Table 4. Comparison of Metrical Parameters and $^{31}P\{^1H\}$ NMR Chemical Shifts of $L^1$ and $L^2$ Complexes**

| metal complex | Pd−P (Å) | P−Pd−P (°) | $^{31}P$ NMR shift |
|---|---|---|---|
| $L^1PdCl_2$ | 2.3311(13), 2.2742(13) | 100.02(5) | 38.47 |
| $L^2PdCl_2$ | 2.3372(6), 2.3483(6) | 162.72(2) | 28.64 |
| $L^1Pd(OAc)_2$ | 2.2759(7), 2.2486(8) | 101.06(3) | 34.62 |
| $L^2Pd(OAc)_2$ | 2.3575(10) | 163.31(6) | 18.31 |
| $L^1Pd(dba)$ | 2.3953(13), 2.3337(13) | 113.33(5) | 21.53, 20.69 |
| $L^2Pd(dba)$ | 2.3390(5), 2.3473(5) | 117.117(17) | 32.89, 19.48 |

## EXPERIMENTAL SECTION

**General Remarks.** Experiments were performed under a dry nitrogen atmosphere using GloveBox techniques. Solvents were dried by passing through a column of activated alumina, followed by storage under dinitrogen. All commercial chemicals were used as received, unless specified otherwise. (COD)$PdCl_2$ and $Pd(OAc)_2$ were purchased from Sigma−Aldrich. Deuterated solvents were obtained from Cambridge Isotope Laboratories. $CD_2Cl_2$ and $CDCl_3$ were dried over molecular sieved, while $C_6D_6$ was dried by stirring over dry $CaH_2$ and filtered prior to use. $L^1$ and 1,2-bis(2-bromophenyl)ethane were synthesized following a reported procedure.[43,45,46] NMR spectra were recorded on a Varian 300 or Bruker 400 spectrometer at ambient probe temperature, unless otherwise indicated. Chemical shifts are reported in ppm, relative to residual internal protonated solvent for $^1H$ and $^{13}C\{^1H\}$ NMR spectra or with respect to a $Me_4Si$ standard, when using $CDCl_3$ for the coupling experiments. ESI-MS were recorded at the ND Mass Spectrometry (MS) & Proteomics Facility at the University of Notre Dame. CHN analyses were performed on a CE-440 Elemental Analyzer.

**Synthesis of $L^2$.** 12.8 g (37.64 mmol, 340.06 g $mol^{-1}$) of 1,2-bis(2-bromophenyl)ethane[46] was dissolved in 40 mL of $Et_2O$, and 47.05 mL of $^n$BuLi 1.6 M (75.28 mmol) was added dropwise to the cooled solution. After stirring for 3 h at −78 °C, the conversion to the corresponding dilithiated species was complete. Then, 12 mL of $^iPr_2PCl$ (75.28 mmol) was added dropwise to the stirring solution and allowed to react overnight. The volatiles were removed under reduced pressure and the residue was dissolved in $CH_2Cl_2$. The solution was filtered through Celite and concentrated under reduced pressure. The product was isolated after crystallization from this concentrated $CH_2Cl_2$ solution at −35 °C. The reaction afforded 1,2-bis(2-(diisopropylphosphanyl)phenyl)ethane ($L^2$) in 94% yield, 15.6 g (35.38 mmol, 414.55 g $mol^{-1}$). Analytically pure $L^2$ was obtained by recrystallization from a saturated $CH_2Cl_2$ solution at −35 °C, in 87%


dx.doi.org/10.1021/ic5010566 | Inorg. Chem. 2014, 53, 8517−8528

yield, producing 12.76 g of $L^2$ (30.78 mmol, 4140.55 g $mol^{-1}$). $^1H$ NMR (300 MHz, $C_6D_6$): $\delta$ 7.62 (ddd, $J_{HP}$ = 10.0, $J_{HH}$ = 5.5, $J_{HH}$ = 1.9 Hz, 2H, Ar*H*), 7.41−7.36 (m, 2H, Ar*H*), 7.21 (td, $J_{HP}$ = 9.9 Hz, $J_{HH}$ = 2.1 Hz, 2H, Ar*H*), 7.13 (td, $J_{HP}$ = 9.9, $J_{HH}$ = 2.1 Hz, 2H, Ar*H*), 3.69 (t, $J_{HP}$ = 1.7 Hz, 4H, $-CH_2-CH_2-$), 2.02 (heptd, $J_{HP}$ = 9.3 Hz, $J_{HH}$ = 3.0 Hz, 4H, $-CH(CH_3)_2$), 1.17 (dd, $J$ = 19.8, 9.3 Hz, 6H, $-CH(CH_3)_2$), 0.98 (dd, $J$ = 15.4, 9.3 Hz, 6H, $-CH(CH_3)_2$). $^{13}C$ NMR (75 MHz, $C_6D_6$): $\delta$ 149.81 (d, $J_{CP}$ = 26.0 Hz, Ar*C*), 134.52 (d, $J_{CP}$= 20.0 Hz, Ar*C*), 132.79 (d, $J_{CP}$= 3.0 Hz, Ar*C*), 130.21 (m, Ar, Ar*C*), 129.21 (s, *C*H, Ar*C*), 125.88 (s, *C*H, Ar*C*), 38.20 (dd, $J_{CP}$ = 2.53, 23.12 Hz, $-CH_2-CH_2-$), 24.82 (d, $J_{CP}$ = 13.8 Hz, $-CH(CH_3)_2$), 20.70 (d, $J_{CP}$ = 20.2 Hz, $-CH(CH_3)_2$), 19.75 (d, $J_{CP}$ = 10.9 Hz, $-CH(CH_3)_2$), 16.21 (s, $-CH(CH_3)_2$), 15.07 (d, $J_{CP}$ = 3.2 Hz, $-CH(CH_3)_2$). $^{31}P$ NMR (121 MHz, $C_6D_6$) $\delta$ −6.81.

**Synthesis of $L^1PdCl_2$.** In a 20-mL scintillation vial, 240 mg of $L^1$ ($C_{25}H_{38}P_2$, 400.53 g $mol^{-1}$, 0.60 mmol) was dissolved in a minimum amount of THF and left stirring for 5 min at room temperature (RT). Independently, 165 mg of $Pd(COD)Cl_2$ (99% purity, 285.51 g $mol^{-1}$, 0.57 mmol) was suspended in THF and stirred for 2 min prior to addition to the $L^1$ solution. The reaction turns yellow within 15 min and aliquots of the reaction mixture show that the reaction is complete after 2 h (by $^1H$ and $^{31}P$ NMR). The slight excess of $L^1$ used (5%) was removed at the end of the reaction by *n*-pentane trituration (3 times) and removal of the *n*-pentane solution. After removing the volatiles under reduced pressure for 1 h, 326 mg of $L^1PdCl_2$ ($C_{25}H_{38}Cl_2P_2Pd$, 577.85 g $mol^{-1}$, 0.56 mmol) was obtained in 99% yield. $L^1PdCl_2$ is insoluble in *n*-pentane, so trituration led to no product loss. Recrystallization of $L^1PdCl_2$ can be performed by layering a saturated $CH_2Cl_2$ solution with a small amount of *n*-pentane at −35 °C, in 86% yield. $^1H$ NMR (400 MHz, $CD_2Cl_2$): $\delta$ 7.59 (t, $J_{HP}$ = 6.3 Hz, 2H, Ar*H*), 7.56 (dd, $J_{HP}$ = 5.9, $J_{HH}$ = 3.5 Hz, 2H, Ar*H*), 7.50 (t, $J_{HP}$ = 6.0 Hz, 2H, Ar*H*), 7.39 (tt, $J_{HP}$ = 6.0, $J_{HH}$ = 1.1 Hz, 2H, Ar*H*), 6.95 (dt, $J_{HH}$ = 11.9, $J_{HP}$ = 2.1 Hz, *endo* backbone $-CH_2-$), 4.11 (d, $J_{HH}$ = 11.9 Hz, *exo* backbone $-CH_2-$), 3.79 (dq, $J$ = 11.6, 5.8 Hz, 2H, $-CH(CH_3)_2$), 2.08−1.61 (br s, 2H, $-CH(CH_3)_2$), 1.57 (dd, $J$ = 12.2, 5.7 Hz, 6H, $-CH(CH_3)_2$), 1.44 (d, $J$ = 6.6 Hz, 6H, $-CH(CH_3)_2$), 1.36 (dd, $J$ = 14.0, 5.2 Hz, 6H, $-CH(CH_3)_2$), 0.92 (br s, 6H, $-CH(CH_3)_2$). $^{13}C$ NMR (75 MHz, $CD_2Cl_2$): $\delta$ 145.44 (d, $J_{CP}$ = 12.28 Hz, Ar*C*), 141.37 (br s, Ar*C*), 133.37 (d, $J_{CP}$ = 8.1 Hz, Ar*C*), 131.90 (s, Ar*C*), 131.55 (d, $J_{CP}$ = 1.7 Hz, Ar*C*), 126.98 (d, $J_{CP}$ = 6.5 Hz, Ar*C*), 44.09 (t, $J_{CP}$ = 10.4 Hz, backbone $-CH_2-$), 29.32 (s, $-CH(CH_3)_2$), 28.90 (s, $-CH(CH_3)_2$), 25.55 (d, $J_{CP}$ = 2.1 Hz, $-CH(CH_3)_2$), 25.25 (d, $J_{CP}$ = 0.9 Hz, $-CH(CH_3)_2$), 21.50 (br s, $-CH(CH_3)_2$), 21.33 (d, $J_{CP}$ = 2.9 Hz, $-CH(CH_3)_2$), 20.83 (d, $J_{CP}$ = 1.4 Hz, $-CH(CH_3)_2$). In H-coupled $^{13}C$, the backbone $-CH_2-$ appears as a triplet at 44.05 ppm $J_{CH}$ = 125.95 Hz (spectrum taken on a Varian 300, 14 000 scans). $^{31}P$ NMR (121 MHz, $CD_2Cl_2$): $\delta$ 38.47 (br s). MS (QTOF) *m*/*z*: $C_{25}H_{39}P_2Pd^+$, 505.65 (expected 505.12, loss of $-Cl^-$ and −HCl). Anal. Calcd for $C_{25}H_{38}Cl_2P_2Pd$: C, 51.96; H, 6.63. Found: C, 52.08; H, 6.72.

**Synthesis of $L^2PdCl_2$.** In a 20-mL scintillation vial, 250 mg of $L^2$ ($C_{26}H_{40}P_2$, 414.55 g $mol^{-1}$, 0.60 mmol) was dissolved in a minimum amount of THF and left stirring for 5 min at RT. Independently, 132 mg of $Pd(OAc)_2$ 98% (224.51 g $mol^{-1}$, 0.59 mmol) was suspended in THF and stirred for 2 min prior to dropwise addition to the $L^2$ solution. The reaction turns yellow within 10 min and aliquots of the reaction mixture show that the reaction is complete after 2 h (by $^1H$ and $^{31}P$ NMR). The slight excess of $L^2$ used (5%) was removed at the end of the reaction by *n*-pentane trituration (3 times) and removal of the *n*-pentane solution. After removal of the volatiles under reduced pressure, 324 mg $L^2PdCl_2$ ($C_{26}H_{40}Cl_2P_2Pd$, 591.87 g $mol^{-1}$, 0.54 mmol) was obtained in 95% yield. Recrystallization of $L^2PdCl_2$ was achieved by layering a saturated toluene solution of $L^2PdCl_2$ with *n*-pentane at −35 °C, in 81% overall yield. This method allowed growing single crystals. $^1H$ NMR (300 MHz, $C_6D_6$): $\delta$ 7.29 (dtd, $J$ = 4.8, 3.9, 1.0 Hz, 2H, Ar*H*), 7.24−7.15 (m, 4H, Ar*H*), 7.02−6.94 (m, 2H, Ar*H*), 5.23−5.07 (m, 2H, *endo* $-CH_2-$ backbone), 3.20−3.01 (m, 2H, $-CH(CH_3)_2$), 3.04−2.89 (m, 2H, *exo* backbone $-CH_2-$), 2.77−2.60 (m, 2H, $-CH(CH_3)_2$), 1.83 (td, $J$ = 9.8, 7.6 Hz, 6H, $-CH(CH_3)_2$), 1.25 (q, $J$ = 7.5 Hz, 6H, $-CH(CH_3)_2$), 1.16 (dd, $J$ = 13.1, 6.5 Hz, 6H, $-CH(CH_3)_2$), 0.90 (q, $J$ = 7.2 Hz, 6H, $-CH(CH_3)_2$). $^{13}C$ NMR (75 MHz, $C_6D_6$) $\delta$ 145.00 (t, $J_{CP}$ = 6.9 Hz, Ar*C*), 133.41 (t, $J_{CP}$ = 18.7 Hz, Ar*C*), 131.67 (t, $J_{CP}$ = 3.9 Hz, Ar*C*), 130.98 (s, Ar*C*), 130.25 (s, Ar*C*), 125.89 (t, $J_{CP}$ = 3.1 Hz, Ar*C*), 40.51 (t, $J_{CP}$ = 4.3 Hz, $-CH_2-$), 26.56 (t, $J_{CP}$ = 10.4 Hz, $-CH(CH_3)_2$), 24.14−23.83 (m, $-CH(CH_3)_2$), 19.25 (d, $J_{CP}$ = 6.35 Hz, $-CH(CH_3)_2$), 19.03 (s, $-CH(CH_3)_2$). $^{31}P$ NMR (121 MHz, $C_6D_6$): $\delta$ 28.64 (s). MS (QTOF) *m*/*z*: $C_{26}H_{41}P_2Pd^+$, 519.13 (expected 519.67, loss $Cl^-$ and HCl). Anal. Calcd for $C_{26}H_{40}Cl_2P_2Pd$: C, 52.76; H, 6.81. Found: C, 52.55; H, 6.64.

**Synthesis of $L^1Pd(OAc)_2$.** In a 20-mL scintillation vial, 240 mg of $L^1$ ($C_{25}H_{38}P_2$, 400.53 g $mol^{-1}$, 0.60 mmol) was dissolved in a minimum amount of THF and left stirring for 5 min at RT. Independently, 131 mg of $Pd(OAc)_2$ (98% purity, 0.57 mmol, 224.51 g $mol^{-1}$) was suspended in THF and stirred for 5 min prior to addition to the $L^1$ solution. The reaction turns yellow within 5 min (the $Pd(OAc)_2$ suspension is orange and the $L^1$ solution is colorless) and aliquots of the reaction mixture show that the reaction is complete after 2 h (by $^1H$ and $^{31}P$ NMR). The slight excess of $L^1$ used (5%) was removed at the end of the reaction by *n*-pentane trituration (3 times) and removal of the *n*-pentane solution. After removal of the volatiles under reduced pressure, 331 mg $L^1Pd(OAc)_2$ ($C_{29}H_{44}O_4P_2Pd$, 0.53 mmol 625.03 g $mol^{-1}$) was obtained in 93% yield. Recrystallization of $L^1Pd(OAc)_2$ can be achieved by layering a saturated $CH_2Cl_2$ or toluene solution with a small amount of *n*-pentane at −35 °C, in 76% yield. This method allowed growing single crystals. $^1H$ NMR (300 MHz, $C_6D_6$): $\delta$ 8.04 (dt, $J$ = 14.9, 2.3 Hz, 1H, backbone $-CH(H)$-, *endo*), 7.15−7.07 (m, 2H, Ar*H*), 6.97 (td, $J$ = 7.3, 1.9 Hz, 4H, Ar*H*), 6.83 (t, $J$ = 7.4 Hz, 2H, Ar*H*), 3.89 (d, $J$ = 15.0 Hz, 1H, backbone $-CH(H)-$, *exo*), 3.09−2.74 (m, 2H, $-CH(CH_3)_2$), 2.14 (s, 6H, $-CH_3COO$), 1.67 (dd, $J$ = 16.2, 7.0 Hz, 6H, $-CH(CH_3)_2$), 1.30 (d, $J$ = 3.1 Hz, 2H, $-CH(CH_3)_2$), 1.17 (dd, $J$ = 14.0, 5.4 Hz, 6H, $-CH(CH_3)_2$)), 1.05 (dd, $J$ = 16.5, 7.0 Hz, 6H, $-CH(CH_3)_2$)), 0.67 (d, $J$ = 8.0 Hz, 6H, $-CH(CH_3)_2$). $^{13}C$ NMR (75 MHz, $CDCl_3$): $\delta$ 176.74 (s, $CH_3COO$), 145.83 (d, $J_{CP}$ = 11.8 Hz, Ar*C*), 133.00 (d, $J_{CP}$ = 8.2 Hz, Ar*C*), 131.70 (s, Ar*C*), 131.07 (d, $J_{CP}$ = 2.0 Hz, Ar*C*), 127.37 (d, $J_{CP}$ = 38.3 Hz, Ar*C*), 125.85 (d, $J_{CP}$ = 6.6 Hz, Ar*C*), 42.66 (t, $J_{CP}$ = 10.1 Hz, backbone $-CH_2-$), 25.61 (d, $J_{CP}$ = 28.6 Hz, $-CH(CH_3)_2$), 24.65 (d, $J_{CP}$ = 24.1 Hz, $-CH(CH_3)_2$), 24.03 (s, $-CH(CH_3)_2$), 20.75 (s, $CH_3COO$), 20.68 (s, $-CH(CH_3)_2$), 19.84 (s, $-CH(CH_3)_2$), 19.45 (s, $-CH(CH_3)_2$). $^{31}P$ NMR (121 MHz, $C_6D_6$): 34.62 (br s). MS (QTOF) *m*/*z*: $C_{25}H_{39}P_2Pd^+$, 505.12 (loss $AcO^-$, AcOH, expected 505.00). Anal. Calcd for $C_{29}H_{44}O_4P_2Pd$: C, 55.73; H, 7.10. Found: C, 55.02; H, 7.02.

**Synthesis of $L^2Pd(OAc)_2$.** In a 20-mL scintillation vial, 248 mg of $L^2$ ($C_{26}H_{40}P_2$, 414.55 g $mol^{-1}$, 0.60 mmol) was dissolved in a minimum amount of THF and left stirring for 15 min at RT. Independently, 131 mg of $Pd(OAc)_2$ (98% purity, 0.57 mmol, 224.51 g $mol^{-1}$) was suspended in THF and stirred for 5 min prior to addition to the $L^2$ solution. The reaction turns yellow within 5 min ($Pd(OAc)_2$ suspension is orange, and the $L^2$ solution is colorless, slightly turbid) and aliquots of the reaction mixture show that the reaction is complete after 2 h (by $^1H$ and $^{31}P$ NMR). The slight excess of $L^2$ used (5%) was removed at the end of the reaction by *n*-pentane trituration (3 times) and removal of the *n*-pentane solution. After removal of the volatiles under reduced pressure, 357 mg $L^2Pd(OAc)_2$ ($C_{30}H_{46}O_4P_2Pd$, 0.53 mmol, 639.06 g $mol^{-1}$) was obtained in 98% yield. Recrystallization of $L^2Pd(OAc)_2$ can be achieved by slow vapor diffusion of diethyl ether or hexanes into a saturated toluene solution at −35 °C, in 86% yield. $^1H$ NMR (300 MHz, $C_6D_6$): $\delta$ 7.38 (ddd, $J$ = 7.6, 3.4, 1.7 Hz, 2H, Ar*H*), 7.23 (td, $J$ = 7.3, 1.1 Hz, 2H, Ar*H*), 7.13 (dtd, $J$ = 4.8, 3.4, 1.5 Hz, 2H, Ar*H*), 7.04 (t, $J$ = 7.4 Hz, 2H, Ar*H*), 5.41−5.26 (m, 2H, $-CH_2-$, *endo*), 3.15−3.00 (m, 2H, $-CH_2-$, *exo*), 2.46 (dt, $J$ = 13.8, 6.7 Hz, 2H, $-CH(CH_3)_2$), 2.29−2.15 (m, 2H, $-CH(CH_3)_2$), 1.91 (s, 6H, $CH_3COO-$), 1.75 (dd, $J$ = 16.1, 8.6 Hz, 6H, $-CH(CH_3)_2$), 1.42 (dd, $J$ = 14.7, 7.3 Hz, 6H, $-CH(CH_3)_2$), 0.94 (dd, $J$ = 14.6, 7.3 Hz, 6H, $-CH(CH_3)_2$), 0.67 (dd, $J$ = 12.7, 6.4 Hz, 6H, $-CH(CH_3)_2$). $^{13}C$ NMR (75 MHz, $C_6D_6$): $\delta$ 176.16 (s, $CH_3COO-$), 147.82 (t, $J_{CP}$ = 7.2 Hz, Ar*C*), 132.64 (s, Ar*C*), 132.25 (t, $J_{CP}$ = 3.8 Hz, Ar*C*), 130.49 (s, Ar*C*), 127.30 (t, $J_{CP}$ = 14.3 Hz, Ar*C*), 125.70 (t, $J_{CP}$ = 2.7 Hz, Ar*C*), 41.55 (t, $J_{CP}$ = 4.3 Hz, backbone $-CH_2-$), 24.41 (t, $J_{CP}$ = 10.1 Hz, $-CH(CH_3)_2$), 23.86 (s, $-CH_3COO$), 22.77 (t, $J_{CP}$ = 11.1 Hz,


dx.doi.org/10.1021/ic5010566 | *Inorg. Chem.* 2014, 53, 8517−8528

−CH($CH_3$)$_2$), 19.79 (s, −CH($CH_3$)$_2$), 19.10 (m, −CH($CH_3$)$_2$), 18.99 (s, −CH($CH_3$)$_2$), 16.94 (s, −CH($CH_3$)$_2$). $^{31}$P NMR (121 MHz, $C_6D_6$): $\delta$ 18.31 (s). Anal. Calcd for $C_{30}H_{46}O_4P_2Pd$: C, 56.38; H, 7.26. Found: C, 56.61; H, 7.16.

**Synthesis of L$^1$Pd(dba).** In a 20-mL scintillation vial, 240 mg of L$^1$ ($C_{25}H_{38}P_2$, 400.53 g mol$^{-1}$, 0.60 mmol) was dissolved in THF and left stirring for 5 min at RT. Over the stirring L$^1$ solution, 344 mg Pd(dba)$_2$ (0.60 mmol, 575.00 g mol$^{-1}$) suspended in THF were added dropwise. The reaction turns dark orange and aliquots of the reaction mixture show that the reaction is incomplete after 12 h (by $^1$H and $^{31}$P NMR). After an additional 24 h, the volatiles were removed under reduced pressure and multiple triturations (hexanes and Et$_2$O) were carried out to obtain L$^1$Pd(dba) in 53% yield (0.32 mmol, 234 mg). L$^1$Pd(dba) ($C_{42}H_{52}OP_2Pd$, 741.23 g mol$^{-1}$) was crystallized from a toluene solution layered with diethyl ether. Traces of uncoordinated dba could be observed by $^1$H NMR spectroscopy in the aryl region. $^1$H NMR (500 MHz, $C_6D_6$, 279 K): $\delta$ 7.97 (d, $J$ = 15.2 Hz, 1H, −C*H*═CH−CO uncoordinated, dba), 7.48 (dd, $J$ = 19.6, 6.5 Hz, 2H, Ar*H*), 7.39 (s, 1H, Ar*H*), 7.25−7.17 (m, 2H, Ar*H*), 7.17−6.95 (m, 12H, Ar*H*), 6.93−6.86 (m, 1H, −CH═C*H*−CO uncoordinated, dba), 6.83−6.73 (m, 2H, backbone −C*H*(H)− and Ar*H*), 5.36 (br s, 1H, −C*H*═CH−CO coordinated, dba), 4.76 (br s, 1H, −CH═C*H*−CO coordinated, dba), 3.00 (d, $J$ = 13.1 Hz, 1H, backbone −CH(*H*)−), 1.88−1.78 (m, 1H, −C*H*($CH_3$)$_2$), 1.54 (dd, $J$ = 14.1, 5.0 Hz, 3H, −CH(C*H*$_3$)$_2$), 1.46−1.32 (m, 1H, −C*H*($CH_3$)$_2$), 1.27 (dd, $J$ = 16.3, 4.9 Hz, 3H, −CH(C*H*$_3$)$_2$), 1.17 (dd, $J$ = 16.5, 6.3 Hz, 3H, −CH(C*H*$_3$)$_2$), 1.13−1.07 (m, 3H, −CH(C*H*$_3$)$_2$), 1.01 (dd, $J$ = 17.9, 5.4 Hz, 3H, −CH(C*H*$_3$)$_2$), 0.86 (m, 1H, −C*H*($CH_3$)$_2$),0.69 (s, 1H, −C*H*($CH_3$)$_2$), 0.55 (t, $J$ = 7.5 Hz, 3H, −CH(C*H*$_3$)$_2$), 0.25 (dd, $J$ = 16.4, 6.4 Hz, 3H, −CH(C*H*$_3$)$_2$), 0.10 (dd, $J$ = 15.2, 6.3 Hz, 3H, −CH(C*H*$_3$)$_2$). $^{31}$P NMR (162 MHz, $C_6D_6$, 279 K): $\delta$ 21.53 (d, $J_{PP}$ = 6.5 Hz), 20.69 (s, br). $^{13}$C NMR (126 MHz, $C_6D_6$, 279 K): $\delta$ 187.96 (dd, $J_{CP}$ = 2.21, 3.01 Hz, C═O), 148.28 (d, $J_{CP}$ = 16.7 Hz, ArC), 147.55 (d, $J_{CP}$ = 16.9 Hz, ArC), 145.31 (d, $J_{CP}$ = 6.6 Hz, ArC), 142.64 (s, ArC), 137.92 (s, ArC); 136.90 (s, ArC), 133.26 (s, ArC), 132.59 (d, $J_{CP}$ = 10.4 Hz, ArC), 131.92 (d, $J_{CP}$ = 5.0 Hz, Ar*C*), 131.51 (d, $J_{CP}$ = 5.8 Hz, −*C*H═CH−CO uncoordinated, dba), 130.48 (s, −CH═*C*H−CO uncoordinated, dba),), 130.19 (s, ArC), 130.07 (d, $J_{CP}$ = 22.3 Hz, ArC), 129.22 (s, Ar*C*), 128.97 (s, −*C*H═CH−CO coordinated, dba), 128.90 (d, $J_{CP}$ = 8.0 Hz, ArC), 128.73 (s, ArC), 128.66 (s, ArC), 128.24 (s, ArC), 128.01 (s, ArC), 127.86 (s, Ar*C*), 126.55 (s, ArC), 126.01 (s, ArC), 125.60 (s, ArC), 125.44 (s, ArC), 124.75 (s, ArC), 124.51 (s, ArC), 124.42 (s, −CH═CH−CO coordinated, dba), 64.37 (d, $J_{PC}$ = 24.0 Hz, backbone −$CH_2$−), 36.78 (dd, $J_{CP}$ = 18.2, 13.9 Hz, −CH($CH_3$)$_2$), 26.29 (dd, $J_{CP}$ = 12.3, 4.7 Hz, −C*H*($CH_3$)$_2$), 25.05 (d, $J_{CP}$ = 14.4 Hz, −CH($CH_3$)$_2$), 23.72 (d, $J_{CP}$ = 16.6 Hz, −CH($CH_3$)$_2$), 21.83 (d, $J_{CP}$ = 10.3 Hz, −CH($CH_3$)$_2$), 20.11 (d, $J_{CP}$ = 6.4 Hz, −CH($CH_3$)$_2$), 19.01 (d, $J_{CP}$ = 5.6 Hz, −CH($CH_3$)$_2$), 18.91 (s, −CH($CH_3$)$_2$)), 18.80 (d, $J_{CP}$ = 6.9 Hz, −CH($CH_3$)$_2$), 18.26 (d, $J_{CP}$ = 8.8 Hz, −CH($CH_3$)$_2$), 17.33 (d, $J_{CP}$ = 6.8 Hz, −CH($CH_3$)$_2$), 16.01 (d, $J_{CP}$ = 7.2 Hz, −CH($CH_3$)$_2$). MS (QTOF) $m/z$: $C_{25}H_{39}P_2Pd^+$, 507.12 (expected 507.57, loss of dba). Anal. Calcd for $C_{42}H_{52}OP_2Pd$: C, 68.06; H, 7.07. Found: C, 67.98; H, 6.93.

**Synthesis of L$^2$Pd(dba).** In a 20-mL scintillation vial, 248 mg of L$^2$ ($C_{26}H_{40}P_2$, 414.55 g mol$^{-1}$, 0.60 mmol) was dissolved in a minimum amount of THF and left stirring for 5 min at RT. 344 mg Pd(dba)$_2$ (0.60 mmol, 575.00 g mol$^{-1}$) suspended in THF was added dropwise to the stirring L$^2$ solution. The reaction turns dark orange and aliquots of the reaction mixture show that the reaction is incomplete after 12 h (by $^1$H and $^{31}$P NMR). After an additional 24 h, the volatiles were removed under reduced pressure and multiple triturations (hexanes and Et$_2$O) were carried out to obtain L$^2$Pd(dba) in 42% yield (0.25 mmol, 186 mg). L$^2$Pd(dba) ($C_{43}H_{54}OP_2Pd$, 755.26 g mol$^{-1}$) was crystallized from a toluene solution layered with diethyl ether. Traces of uncoordinated dba could be observed by $^1$H NMR spectroscopy in the aryl region. The room temperature $^1$H NMR was broad in $C_6D_6$. $^1$H NMR (400 MHz, toluene-d$_8$, 260 K) $\delta$ 7.80−7.74 (m, 1H, −C*H*═CH−CO uncoordinated, dba), 7.42 (t, $J$ = 7.6 Hz, 1H, −CH═C*H*−CO uncoordinated, dba), 7.37 (d, $J$ = 7.2 Hz, 2H, Ar*H*), 7.25 (d, $J$ = 7.5 Hz, 2H, Ar*H*), 7.21−7.11 (m, 5H, Ar*H*), 7.06 (dd, $J$ = 15.1, 7.6 Hz, 4H, Ar*H*), 7.00 (t, $J$ = 7.3 Hz, 2H, Ar*H*), 6.95 (d, $J$ = 4.5 Hz, 1H, −C*H*═CH−CO coordinated, dba), 6.91−6.83 (m, 2H, Ar*H*), 6.66 (d, $J$ = 15.28 Hz, 1H, Ar*H*), 6.63 (d, $J$ = 3.8 Hz, 1H, −CH═C*H*-CO coordinated, dba), 4.85−4.77 (m,1H, backbone −C$H_2$−), 4.73 (t, $J$ = 11.2 Hz, 1H, backbone −C$H_2$−), 4.64−4.55 (m, 1H, backbone −C$H_2$−), 3.52 (dd, $J$ = 14.5, 7.2 Hz, 1H, backbone −C$H_2$−), 2.44−2.26 (m, 2H, −C*H*($CH_3$)$_2$), 1.95−1.80 (m, 1H, −C*H*($CH_3$)$_2$), 1.71 (dd, $J$ = 18.1, 7.3 Hz, 3H, −CH(C*H*$_3$)$_2$), 1.33 (t, $J$ = 7.7 Hz, 3H, −CH(C*H*$_3$)$_2$), 1.22 (dd, $J$ = 11.8, 5.6 Hz, 1H, −C*H*($CH_3$)$_2$), 1.05 (dd, $J$ = 16.3, 6.9 Hz, 6H, −CH(C*H*$_3$)$_2$), 0.92 (dd, $J$ = 16.14, 6.65 Hz, 3H, −CH(C*H*$_3$)$_2$), 0.61 (dd, $J$ = 16.76, 6.76 Hz, 6H, −CH(C*H*$_3$)$_2$), 0.45 (dd, $J$ = 17.7, 6.6 Hz, 3H, −CH(C*H*$_3$)$_2$). $^{31}$P NMR (202 MHz, toluene-d$_8$, 260 K): $\delta$ 32.89 (br s), 19.48 (d, $J_{PP}$ = 8.0 Hz). $^{13}$C NMR (101 MHz, toluene-d$_8$, 260 K): $\delta$ 186.10 (t, $J_{CP}$ = 4.1 Hz, C═O), 149.25 (d, $J_{CP}$ = 15.0 Hz, Ar*C*), 145.00 (d, $J_{CP}$ = 6.4 Hz, ArC), 142.74 (d, $J_{CP}$ = 13.2 Hz, ArC), 142.51 (s, ArC), 141.84 (d, $J_{CP}$ = 12.9 Hz, ArC), 137.84 (s, ArC), 136.40 (s, ArC), 136.31 (d, $J_{CP}$ = 18.6 Hz, Ar*C*), 135.01 (s, Ar*C*), 132.55 (s, −*C*H═CH−CO uncoordinated, dba), 131.14 (s, −CH═*C*H−CO uncoordinated, dba), 130.90 (d, $J_{CP}$ = 16.1 Hz, Ar*C*), 130.19 (d, $J_{CP}$ = 5.6 Hz, -*C*H═CH−CO coordinated, dba), 130.19−130.12 (m, Ar*C*), 129.39 (s, Ar*C*), 129.01 (s, ArC), 128.83 (s, ArC), 128.57 (s, Ar*C*), 128.35 (s, ArC), 128.09 (s, ArC), 127.99 (s, ArC), 127.73 (s, ArC), 126.73 (s, ArC), 125.72 (s, ArC), 125.69 (s, ArC), 125.09 (d, $J_{CP}$ = 2.4 Hz, ArC), 124.49 (d, $J_{CP}$ = 2.4 Hz, −CH═CH−CO coordinated, dba), 121.45 (s, Ar*C*), 75.48 (dd, $J_{CP}$ = 16.8, $J_{CP}$ = 5.6 Hz, backbone −*C*H$_2$−), 64.74 (dd, $J_{CP}$ = 25.8, $J_{CP}$ = 2.6 Hz, backbone −CH$_2$−), 41.06 (d, $J_{CP}$ = 7.9 Hz, −CH($CH_3$)$_2$), 38.20 (d, $J_{CP}$ = 18.7 Hz, −C*H*($CH_3$)$_2$), 24.73 (dd, $J_{CP}$ = 15.7, 7.0 Hz, −C*H*($CH_3$)$_2$), 24.29 (d, $J_{CP}$ = 17.2 Hz, −CH($CH_3$)$_2$), 21.55 (d, $J_{CP}$ = 15.8 Hz, −CH(*C*H$_3$)$_2$), 20.61 (s, −CH($CH_3$)$_2$), 19.77 (s, −CH(*C*H$_3$)$_2$), 19.66 (d, $J_{CP}$ = 9.5 Hz, −CH(*C*H$_3$)$_2$), 19.16 (d, $J_{CP}$ = 6.3 Hz, −CH(*C*H$_3$)$_2$), 19.01 (d, $J_{CP}$ = 7.3 Hz, −CH(*C*H$_3$)$_2$), 18.13 (d, $J_{CP}$ = 15.5 Hz, −CH(*C*H$_3$)$_2$), 15.43 (d, $J_{CP}$ = 7.1 Hz, −CH(*C*H$_3$)$_2$). Anal. Calcd for $C_{43}H_{54}OP_2Pd$: C, 68.38; H, 7.21. Found: C, 68.58; H, 7.20.

**Synthesis of [L$^2$Rh(nbd)]BF$_4$.** In a 20-mL scintillation vial, 33 mg of L$^2$ ($C_{26}H_{40}P_2$, 414.55 g mol$^{-1}$, 0.08 mmol) was dissolved in a minimum amount of THF and cooled at −60 °C in the cold well. Independently, 30 mg of [Rh(nbd)$_2$]BF$_4$ (99% purity, 0.08 mmol, 375 g mol$^{-1}$) was suspended in THF and stirred for 5 min prior to addition to the L$^2$ solution. The color of the solution changed from orange-red (suspension of Rh$^+$ precursor is red) to light orange and finally yellow after stirring for 1 h and subsequent warming up to RT. Trituration with *n*-pentane was repeated twice in order to remove any impurities. After solvent removal and trituration, the [L$^2$Rh(nbd)]BF$_4$ ($C_{33}H_{48}BF_4P_2Rh$, 50 mg, 696.39 g mol$^{-1}$) yield was 91%. Recrystallization of [L$^2$Rh(nbd)]BF$_4$ can be achieved by slow vapor diffusion of hexanes into a saturated $CH_2Cl_2$ solution at −35 °C, isolated yield = 73%. $^1$H NMR (500 MHz, $CD_2Cl_2$) $\delta$ 7.45−6.80 (m, 10H, Ar*H* 8H and 2H −C*H*(H)−C*H*(H)−), 5.07 (s, 4H, −C*H*−, nbd), 4.05 (s, 2H, −C*H*−, nbd), 4.04−3.84 (m, 2H, −CH(*H*)−CH(*H*)−), 3.52−2.96 (m, 2H, −C*H*($CH_3$)$_2$), 2.84−2.44 (m, 2H, −C*H*($CH_3$)$_2$), 2.40−2.00 (m, 2H, −C$H_2$−, nbd), 1.85−1.65 (m, 3H, −CH(C*H*$_3$)$_2$), 1.45 (s, 9H, −CH(C*H*$_3$)$_2$), 1.17−0.89 (m, 6H, −CH(C*H*$_3$)$_2$), 0.83−0.41 (m, 6H, −CH(C*H*$_3$)$_2$). $^{13}$C NMR (126 MHz, $CD_2Cl_2$): $\delta$ 144.28 (s, ArC), 132.50 (s, ArC), 130.74 (s, Ar*C*), 130.46 (s, ArC), 127.39 (s, ArC), 126.37 (s, Ar*C*), 72.69 (s, nbd*C*), 70.83 (s, nbd*C*), 68.31 (s, nbd*C*), 52.29 (s, nbd*C*), 36.14 (s, backbone −CH$_2$−CH$_2$−), 23.70 (d, $J_{CP}$ = 18.8 Hz, −CH($CH_3$)$_2$), 21.74 (s, −CH($CH_3$)$_2$), 20.94 (s, −CH($CH_3$)$_2$), 20.48 (s, −CH($CH_3$)$_2$), 20.13 (s, −CH($CH_3$)$_2$), 17.77 (s, −CH($CH_3$)$_2$). $^{31}$P NMR (202 MHz, $CD_2Cl_2$) $\delta$ 21.98 (d, $J_{RhP}$ = 119.6 Hz). $^{19}$F NMR (471 MHz, $CD_2Cl_2$) $\delta$ −158.76 (s). MS (QTOF) $m/z$: $C_{33}H_{48}P_2Rh^+$, 609.20 (expected 609.22, loss of $BF_4^-$); $C_{26}H_{40}P_2Rh^+$, 517.00 (expected 517.16, additional loss of nbd ligand). Anal. Calcd for $C_{33}H_{48}BF_4P_2Rh\cdot 0.5CH_2Cl_2$: C, 54.82, H, 6.63. Found: C, 54.70, H, 6.59.

**Synthesis of [L$^1$Pd]$_2$.** To a solution of 58 mg of L$^1$PdCl$_2$ ($C_{25}H_{38}Cl_2P_2Pd$, MW: 577.85 g mol$^{-1}$, 0.10 mmol) in THF, a suspension of Mg (6 mg, 250% of the stoichiometric amount, 0.25 mmol) in THF was added at ambient temperature and stirred


dx.doi.org/10.1021/ic5010566 | Inorg. Chem. 2014, 53, 8517−8528

overnight. The reaction mixture turned orange-gray; then, it was filtered over Celite and the volatiles were removed under reduced pressure. The same product could be obtained from the reaction of $L^1PdCl_2$ with 1.5 or 2 equiv $Li[(C_2H_5)_3BH]$ at low temperature (−80 °C) for 4 h and allowing the reaction mixture to warm up to RT, followed by a similar workup. Using 1 equiv of $Li(C_2H_5)_3BH$, the major product (65% by NMR spectroscopy) is still $[L^1Pd]_2$, but there is evidence of an unsymmetrical side-product (2 doublets in the $^{31}P$ NMR spectrum). The orange powder was washed three times with *n*-pentane, and the volatiles were removed under reduced pressure. The product was recrystallized from a saturated *n*-pentane solution in 74% yield, as an orange crystalline powder. $^1H$ NMR (300 MHz, $C_6D_6$): $\delta$ 7.36 (s, 2H, backbone $-CH_2-$), 7.27 (m, 4H, Ar*H*), 7.06 (td, $J$ = 7.6, 1.2 Hz, 2H, Ar*H*), 6.97 (td, $J$ = 7.5, 1.3 Hz, 2H, Ar*H*), 2.24−2.10 (m, 2H, $-CH(CH_3)_2$), 2.06−1.93 (m, 2H, $-CH(CH_3)_2$), 1.49 (dd, $J$ = 15.6, 7.0 Hz, 6H, $-CH(CH_3)_2$), 1.28 (ddd, $J$ = 14.2, 13.8, 6.9 Hz, 12H, $-CH(CH_3)_2$), 0.79 (dd, $J$ = 15.0, 7.0 Hz, 6H, $-CH(CH_3)_2$). $^{13}C$ NMR (101 MHz, $C_6D_6$): $\delta$ 151.60 (t, $J_{CP}$ = 9.0 Hz, Ar*C*), 134.40 (t, $J_{CP}$ = 11.1 Hz, Ar*C*), 132.88 (t, $J_{CP}$ = 2.6 Hz, Ar*C*), 131.90 (s, Ar*C*), 129.27 (s, Ar*C*), 125.18 (t, $J_{CP}$ = 1.8 Hz, Ar*C*), 43.11 (t, $J_{CP}$ = 11.4 Hz, backbone $-CH_2$-), 28.68 (t, $J_{CP}$ = 7.5 Hz, $-CH(CH_3)_2$), 27.73 (t, $J_{CP}$ = 8.3 Hz, $-CH(CH_3)_2$), 22.59 (t, $J_{CP}$ = 7.2 Hz, $-CH(CH_3)_2$), 22.06 (t, $J_{CP}$ = 6.4 Hz, $-CH(CH_3)_2$), 21.39 (t, $J_{CP}$ = 3.5 Hz, $-CH(CH_3)_2$), 21.09 (t, $J_{CP}$ = 4.3 Hz, $-CH(CH_3)_2$). $^{31}P$ NMR (121 MHz, $C_6D_6$): $\delta$ 28.88 (s). Anal. Calcd for $C_{50}H_{76}P_4Pd_2$: C, 59.23; H, 7.56. Found: C, 59.18; H, 7.48.

**Synthesis of $L^2Pd$.** To a THF solution of $L^2PdCl_2$ (59 mg, 591.87 g mol$^{-1}$, 0.10 mmol, $C_{26}H_{40}Cl_2P_2Pd$), a suspension of 6 mg of Mg in THF (0.25 mmol) was added dropwise at ambient temperature and the mixture was stirred overnight. The solution turned gray-yellow and it was filtered through a plug of Celite. The solution obtained was light gray-yellow, and the volatiles were removed under reduced pressure. After successive washings with *n*-pentane in order to remove traces of THF, the product was recrystallized from a saturated *n*-pentane solution, affording $L^2Pd$ as off-gray crystals ($C_{26}H_{40}P_2Pd$, 520.92 g mol$^{-1}$, 52 mg) in 89% yield. Reaction of $L^2PdCl_2$ with 1−2 equiv $Li(C_2H_5)_3BH$ (−80 °C, 4 h) leads to the same product, in 83% yield. $^1H$ NMR: (300 MHz, $C_6D_6$) $\delta$ 7.32−7.17 (m, 6H, Ar*H*), 7.08 (td, $J$ = 7.4, 1.5 Hz, 2H, Ar*H*), 5.95−5.80 (m, 2H, backbone $-CH_2-$, *endo*), 2.65−2.49 (m, 2H, backbone $-CH_2-$, *exo*), 2.18−2.06 (m, 2H, $-CH(CH_3)_2$), 1.98 (dt, $J$ = 14.1, 7.0 Hz, 2H, $-CH(CH_3)_2$), 1.40 (dd, $J$ = 17.1, 6.8 Hz, 6H, $-CH(CH_3)_2$), 1.25 (dt, $J$ = 14.6, 7.3 Hz, 12H, $-CH(CH_3)_2$), 0.83 (dd, $J$ = 11.9, 6.7 Hz, 6H, $-CH(CH_3)_2$). $^{13}C$ NMR: (75 MHz, $C_6D_6$): $\delta$ 149.37 (t, $J_{CP}$ = 8.9 Hz, Ar*C*), 132.59 (s, ipso, Ar*C*), 132.53 (s, Ar*C*), 132.16 (t, $J_{CP}$ = 3.3 Hz, Ar*C*), 129.36 (s, Ar*C*), 125.68 (t, $J_{CP}$ = 1.8 Hz, Ar*C*), 41.58 (t, $J_{CP}$ = 7.1 Hz, backbone $-CH_2-$), 28.44 (t, $J_{CP}$ = 7.0 Hz, $-CH(CH_3)_2$), 24.19 (t, $J_{CP}$ = 8.4 Hz, $-CH(CH_3)_2$), 21.67−21.36 (m, $-CH(CH_3)_2$), 21.24 (t, $J_{CP}$ = 5.9 Hz, $-CH(CH_3)_2$), 18.31 (s, $-CH(CH_3)_2$). $^{31}P$ NMR (121 MHz, $C_6D_6$): 29.85 (s). Anal. Calcd for $C_{26}H_{40}P_2Pd$: C, 59.94; H, 7.74. Found: C, 59.61; H, 7.70.

**Synthesis of $L^2Pd(p\text{-}C_6H_4\text{-}NO_2)Br$.** 52 mg of $L^2Pd$ ($C_{26}H_{40}P_2Pd$, 520.97 g mol$^{-1}$, 0.10 mmol) were mixed in toluene with 20 mg of 1-bromo-4-nitrobenzene ($C_6H_4BrNO_2$, 202.01 g mol$^{-1}$, 0.10 mmol) and stirred for 2 h at RT. The workup consisted solely of solvent removal under reduced pressure and trituration with *n*-pentane. The $^1H$ and $^{31}P$ NMR spectra showed the product to be pure. After recrystallization out of a concentrated toluene solution layered with *n*-pentane, 62 mg of $L^2PdBr(C_6H_4NO_2)$ ($C_{32}H_{44}BrNO_2P_2Pd$, 722.98 g mol$^{-1}$, 0.08 mmol) were isolated in 86% overall yield. This method also afforded X-ray-quality crystals. A control experiment was also carried out in order to follow the ligand dynamics during the oxidative addition process. After 5 min, the conversion was found to be already 86%. The reaction was monitored by $^1H$ and $^{31}P$ spectroscopy, and spectra were recorded every 15 min, up to 1 h when the reaction was found to be virtually complete. Conversion: 86% (5 min); 95% (15 min); 96% (30 min); 97% (45 min); 98% (60 min). No intermediates were observed throughout the experiment. $^1H$ NMR (400 MHz, $C_6D_6$) $\delta$ 7.99 (dt, $J$ = 8.5, 1.7 Hz, 1H, Ar), 7.75 (dd, $J$ = 8.5, 2.7 Hz, 1H, Ar*H*), 7.53 (dd, $J$ = 8.5, 2.7 Hz, 1H, Ar*H*), 7.43 (t, $J$ = 7.4 Hz, 1H, Ar*H*), 7.30−7.18 (m, 4H, Ar*H*), 7.14−7.07 (m, 1H, Ar*H*), 6.90 (ddd, $J$ = 8.8, 4.8, 1.1 Hz, 1H, Ar*H*), 6.74 (t, $J$ = 7.4 Hz, 1H, Ar), 6.10 (d, $J$ = 8.5 Hz, 1H, Ar*H*), 4.56 (t, $J$ = 12.1 Hz, 1H, $-CH(H)-CH_2-$), 4.11 (m, 1H, $-CH(H)-CH(H)-$), 3.68−3.52 (m, 1H, $-CH(CH_3)_2$), 3.38−3.26 (m, 1H, $-CH(CH_3)_2$), 2.90 (td, $J$ = 12.5, 6.8 Hz, 1H, $-CH(H)-CH(H)-$), 2.80 (td, $J$ = 12.8, 6.7 Hz, 1H, $-CH(H)-CH_2-$), 1.81 (dd, $J$ = 20.3, 7.4 Hz, 3H, $-CH(CH_3)_2$), 1.76 (d, $J$ = 3.3 Hz, 1H, $-CH(CH_3)_2$), 1.48 (dd, $J$ = 15.9, 7.2 Hz, 3H, $-CH(CH_3)_2$), 1.36−1.24 (m, 4H, $-CH(CH_3)_2$ and $-CH(CH_3)_2$), 1.15 (ddd, $J$ = 10.0, 7.3, 0.8 Hz, 3H, $-CH(CH_3)_2$), 1.00−0.91 (m, 3H, $-CH(CH_3)_2$), 0.71 (ddd, $J$ = 12.3, 7.5, 1.2 Hz, 3H, $-CH(CH_3)_2$), 0.37−0.29 (m, 3H, $-CH(CH_3)_2$), 0.22 (dd, $J$ = 14.4, 7.2 Hz, 3H, $-CH(CH_3)_2$). $^{13}C$ NMR (101 MHz, $C_6D_6$) $\delta$ 165.67 (dd, $J_{CP}$ = 6.2, 2.5 Hz, Ar*C*), 145.55 (t, $J_{CP}$ = 1.8 Hz, Ar*C*), 144.77 (d, $J_{CP}$ = 12.3 Hz, Ar*C*), 143.04 (d, $J_{CP}$ = 12.5 Hz, Ar*C*), 138.49 (dd, $J_{CP}$ = 5.1, 2.0 Hz, Ar*C*), 136.30 (d, $J_{CP}$ = 1.3 Hz, Ar*C*), 135.85 (dd, $J_{CP}$ = 4.6, 3.0 Hz, Ar*C*), 131.72 (d, $J_{CP}$ = 7.6 Hz, Ar*C*), 131.57 (s, Ar*C*), 131.53 (s, Ar*C*), 131.24 (s, Ar*C*), 130.74 (d, $J_{CP}$ = 7.6 Hz, Ar*C*), 130.59 (d, $J_{CP}$ = 2.4 Hz, Ar*C*), 130.35 (d, $J_{CP}$ = 1.7 Hz, Ar*C*), 129.82 (d, $J_{CP}$ = 1.8 Hz, Ar*C*), 126.06 (dd, $J_{CP}$ = 18.3, 5.5 Hz, Ar*C*), 121.26 (s, Ar*C*), 118.79 (s, Ar*C*), 40.33 (d, $J_{CP}$ = 11.8 Hz, $-CH_2-CH_2-$), 38.61 (d, $J_{CP}$ = 9.6 Hz, $-CH_2-CH_2-$), 29.03 (dd, $J_{CP}$ = 17.8, 4.3 Hz, $-CH(CH_3)_2$), 27.39 (dd, $J_{CP}$ = 16.3, 2.6 Hz, $-CH(CH_3)_2$), 25.96 (dd, $J_{CP}$ = 18.4, 3.6 Hz, $-CH(CH_3)_2$), 24.91 (d, $J_{CP}$ = 13.5 Hz, $-CH(CH_3)_2$), 23.61 (dd, $J_{CP}$ = 17.2, 3.1 Hz, $-CH(CH_3)_2$), 22.98 (d, $J_{CP}$ = 10.6 Hz, $-CH(CH_3)_2$), 20.38 (s, $-CH(CH_3)_2$), 20.14 (dd, $J_{CP}$ = 6.4, 2.9 Hz, $-CH(CH_3)_2$), 19.67 (dd, $J_{CP}$ = 3.2, 2.0 Hz, $-CH(CH_3)_2$), 19.41 (dd, $J_{CP}$ = 5.4, 3.0 Hz, $-CH(CH_3)_2$), 18.98 (dd, $J_{CP}$ = 6.0, 2.8 Hz, $-CH(CH_3)_2$), 17.70 (s, $-CH(CH_3)_2$. $^{31}P$ NMR (162 MHz, $C_6D_6$) $\delta$ 28.55 (d, $J_{PP}$ = 399.6 Hz), 21.23 (d, $J_{PP}$= 399.5 Hz). Anal. Calcd for $C_{32}H_{44}BrNO_2P_2Pd$: C, 53.16; H, 6.13; N 1.94. Found: C, 53.24; H, 6.19; N 1.90.

**Representative Procedure for Suzuki Couplings.**[69] $Cs_2CO_3$ (196 mg, 0.6 mmol), phenylboronic acid (367 mg, 0.3 mmol), bromoacetophenone (40 mg, 0.2 mmol), 1 mol % (relative to aryl halide) of the Pd precatalyst, and the internal standard 1,3,5-trimethoxybenzene (34 mg, 0.2 mmol) in 1,4-dioxane (1.4 mL) were added to a flask equipped with a stir bar, under nitrogen atmosphere. The solution was heated with stirring at 100 °C under $N_2$ for the specified period of time. After cooling, a $^1H$ NMR spectrum of the reaction mixture was acquired in $CDCl_3$. The yield was computed as an average of two runs determined by $^1H$ NMR spectroscopy using an internal standard; only the trans isomer was observed. No increase in yield was observed when the reaction mixture was stirred for longer times.

**Representative Procedure for Heck Couplings.**[70] $^nBu_4NBr$ (13 mg, 0.041 mmol) and $K_2CO_3$ (64 mg, 0.46 mmol), 1-bromo-4-nitrobenzene (84 mg, 0.41 mmol), and a 0.5 mL solution of 0.1 mol % (relative to the aryl halide) Pd precatalyst in dimethylacetamide (DMA), *n*-butyl acrylate (105.6 mg, 0.82 mmol), and the internal standard (1,3,5-trimethoxybenzene, 69 mg, 0.41 mmol, as a 1.5 mL solution in DMA) were combined. The mixture was stirred under $N_2$ at 140 °C for the specified time. After cooling, a $^1H$ NMR spectrum of the reaction mixture was acquired in $CDCl_3$. The yield was computed as an average of two runs determined by $^1H$ NMR spectroscopy using an internal standard; only the trans isomer was observed. No increase in yield was observed when the reaction mixture was stirred for longer times.

**X-ray Crystallography.** The diffraction experiments were carried out on a Bruker AXS SMART CCD three-circle diffractometer with a sealed tube using graphite-monochromated Mo K$\alpha$ radiation ($\lambda$ = 0.71073 Å). The crystals were mounted on a plastic loop and used for the diffraction experiments. Anisotropic thermal parameters were refined for all non-hydrogen atoms. The hydrogens were placed according to a riding model. Details of the crystal structures and refinement data for complexes **1**−**10** are given in the Supporting Information.

**X-ray Crystal Structure of $L^2$.** Single crystals were obtained as colorless blocks from a concentrated *n*-pentane solution at −35 °C in the glovebox. Crystal and refinement data for $L^2$: $C_{26}H_{40}P_2$; $M_r$ = 414.52; triclinic; space group $P\bar{1}$; $a$ = 7.1305(9) Å; $b$ = 7.2635(9) Å; $c$


dx.doi.org/10.1021/ic5010566 | *Inorg. Chem.* 2014, 53, 8517−8528

= 12.7304(17) Å; $\alpha$ = 88.779(2)°; $\beta$ = 78.166(2)°; $\gamma$ = 72.008(2)°; $V$ = 613.14(14) Å$^3$; $Z$ = 1; $T$ = 100(2) K; $\lambda$ = 0.71073 Å; $\mu$ = 0.187 mm$^{-1}$; $d_{calc}$ = 1.123 g cm$^{-3}$; 12 575 reflections collected; 2158 unique ($R_{int}$ = 0.0235); giving $R_1$ = 0.0271, $wR_2$ = 0.0706 for 2056 data with [$I > 2\sigma(I)$] and $R_1$ = 0.0288, $wR_2$ = 0.0721 for all 2158 data. Residual electron density (e$^-$ Å$^{-3}$) max/min: 0.366/−0.174.

**X-ray Crystal Structure of L$^1$PdCl$_2$.** Single crystals were obtained as yellow blocks from a concentrated dichloromethane (DCM) solution layered with *n*-pentane at −35 °C in the glovebox. Crystal and refinement data for L$^1$PdCl$_2$: $C_{25}H_{38}Cl_2P_2Pd$; $M_r$ = 577.79; monoclinic; space group $P2(1)/n$; $a$ = 10.3224(8) Å; $b$ = 15.9598(13) Å; $c$ = 16.8281(14) Å; $\alpha$ = 90°; $\beta$ = 102.4370(10)°; $\gamma$ = 90°; $V$ = 2707.3(4) Å$^3$; $Z$ = 4; $T$ = 120(2) K; $\lambda$ = 0.71073 Å; $\mu$ = 1.012 mm$^{-1}$; $d_{calc}$ = 1.418 g cm$^{-3}$; 34 014 reflections collected; 4763 unique ($R_{int}$ = 0.0829); giving $R_1$ = 0.0532, $wR_2$ = 0.0866 for 4048 data with [$I > 2\sigma(I)$] and $R_1$ = 0.0687, $wR_2$ = 0.0903 for all 4763 data. Residual electron density (e$^-$ Å$^{-3}$) max/min: 0.589/−0.686.

**X-ray Crystal Structure of L$^1$Pd(OAc)$_2$.** Single crystals were obtained as yellow blocks from a concentrated DCM solution layered with *n*-pentane at −35 °C in the glovebox. Crystal and refinement data for L$^1$Pd(OAc)$_2$: $C_{30}H_{46}Cl_2O_4P_2Pd$; $M_r$ = 709.91; monoclinic; space group $P2(1)/n$; $a$ = 9.3254(11) Å; $b$ = 11.7802(13) Å; $c$ = 30.612(4) Å; $\alpha$ = 90°; $\beta$ = 91.014(2)°; $\gamma$ = 90°; $V$ = 3362.4(7) Å$^3$; $Z$ = 4; $T$ = 120(2) K; $\lambda$ = 0.71073 Å; $\mu$ = 0.837 mm$^{-1}$; $d_{calc}$ = 1.402 g cm$^{-3}$; 36 669 reflections collected; 5908 unique ($R_{int}$ = 0.0582); giving $R_1$ = 0.0320, $wR_2$ = 0.0637 for 4685 data with [$I > 2\sigma(I)$] and $R_1$ = 0.0496, $wR_2$ = 0.0674 for all 5908 data. Residual electron density (e$^-$ Å$^{-3}$) max/min: 0.384/−0.408.

**X-ray Crystal Structure of L$^2$PdCl$_2$.** Single crystals were obtained as yellow blocks from a concentrated toluene solution at −35 °C in the glovebox. Crystal and refinement data for L$^2$PdCl$_2$: $C_{26}H_{40}Cl_2P_2Pd$; $M_r$ = 591.82; monoclinic; space group $P2(1)/n$; $a$ = 9.4720(7) Å; $b$ = 13.5331(11) Å; $c$ = 20.7908(18) Å; $\alpha$ = 90°; $\beta$ = 94.265(2)°; $\gamma$ = 90°; $V$ = 2657.7(4) Å$^3$; $Z$ = 4; $T$ = 120(2) K; $\lambda$ = 0.71073 Å; $\mu$ = 1.032 mm$^{-1}$; $d_{calc}$ = 1.479 g cm$^{-3}$; 27 106 reflections collected; 4677 unique ($R_{int}$ = 0.0411); giving $R_1$ = 0.0231, $wR_2$ = 0.0484 for 4015 data with [$I > 2\sigma(I)$] and $R_1$ = 0.0321, $wR_2$ = 0.0504 for all 4677 data. Residual electron density (e$^-$ Å$^{-3}$) max/min: 0.367/−0.349.

**X-ray Crystal Structure of L$^2$Pd(OAc)$_2$.** Single crystals were obtained as orange blocks from a concentrated DCM solution at −35 °C in the glovebox. Crystal and refinement data for L$^2$Pd(OAc)$_2$: $C_{38}H_{55}Cl_2O_4P_2Pd$; $M_r$ = 815.06; monoclinic; space group $P2/n$; $a$ = 10.4111(15) Å; $b$ = 12.9808(18) Å; $c$ = 14.580(2) Å; $\alpha$ = 90°; $\beta$ = 102.458(2)°; $\gamma$ = 90°; $V$ = 1924.1(5) Å$^3$; $Z$ = 2; $T$ = 120(2) K; $\lambda$ = 0.71073 Å; $\mu$ = 0.742 mm$^{-1}$; $d_{calc}$ = 1.407 g cm$^{-3}$; 28 610 reflections collected; 3391 unique ($R_{int}$ = 0.0534); giving $R_1$ = 0.0443, $wR_2$ = 0.0977 for 3106 data with [$I > 2\sigma(I)$] and $R_1$ = 0.0495, $wR_2$ = 0.1000 for all 3391 data. Residual electron density (e$^-$ Å$^{-3}$) max/min: 0.638/−0.997.

**X-ray Crystal Structure of L$^1$Pd(dba).** Single crystals were obtained as orange blocks from a concentrated diethyl ether solution at −35 °C in the glovebox. Crystal and refinement data for L$^1$Pd(dba): $C_{42}H_{52}OP_2Pd$; $M_r$ = 741.18; monoclinic; space group $P2(1)/n$; $a$ = 13.054(3) Å; $b$ = 15.323(3) Å; $c$ = 18.240(4) Å; $\alpha$ = 90°; $\beta$ = 93.755(6)°; $\gamma$ = 90°; $V$ = 3640.5(14) Å$^3$; $Z$ = 4; $T$ = 120(2) K; $\lambda$ = 0.71073 Å; $\mu$ = 0.629 mm$^{-1}$; $d_{calc}$ = 1.352 g cm$^{-3}$; 16 694 reflections collected; 6407 unique ($R_{int}$ = 0.0669); giving $R_1$ = 0.0493, $wR_2$ = 0.1007 for 4631 data with [$I > 2\sigma(I)$] and $R_1$ = 0.0801, $wR_2$ = 0.1135 for all 6407 data. Residual electron density (e$^-$ Å$^{-3}$) max/min: 0.646/−0.868.

**X-ray Crystal Structure of L$^2$Pd(dba).** Single crystals were obtained as orange blocks from a concentrated diethyl ether solution at −35 °C in the freezer in the glovebox. Crystal and refinement data for L$^2$Pd(dba): $C_{43}H_{54}OP_2Pd$; $M_r$ = 755.20; monoclinic; space group $P2(1)$; $a$ = 9.8272(4) Å; $b$ = 18.7287(9) Å; $c$ = 10.3022(5) Å; $\alpha$ = 90°; $\beta$ = 90.438(2)°; $\gamma$ = 90°; $V$ = 1896.07(15) Å$^3$; $Z$ = 2; $T$ = 120(2) K; $\lambda$ = 0.71073 Å; $\mu$ = 0.606 mm$^{-1}$; $d_{calc}$ = 1.323 g cm$^{-3}$; 27 576 reflections collected; 8880 unique ($R_{int}$ = 0.0275); giving $R_1$ = 0.0217, $wR_2$ = 0.0453 for 8498 data with [$I > 2\sigma(I)$] and $R_1$ = 0.0238, $wR_2$ = 0.0462 for all 8880 data. Residual electron density (e$^-$ Å$^{-3}$) max/min: 0.254/−0.294.

**X-ray Crystal Structure of [L$^2$Rh(nbd)]BF$_4$.** Single crystals were obtained as yellow blocks from a concentrated DCM solution at −35 °C in the glovebox. Crystal and refinement data for [L$^2$Rh(nbd)]BF$_4$: $C_{33}H_{48}BF_4P_2Rh$; $M_r$ = 696.37; orthorhombic; space group $Pbca$; $a$ = 17.0147(14) Å; $b$ = 17.9627(15) Å; $c$ = 20.3387(17) Å; $\alpha$ = 90°; $\beta$ = 90°; $\gamma$ = 90°; $V$ = 6216.1(9) Å$^3$; $Z$ = 8; $T$ = 120(2) K; $\lambda$ = 0.71073 Å; $\mu$ = 0.699 mm$^{-1}$; $d_{calc}$ = 1.488 g cm$^{-3}$; 52 131 reflections collected; 6222 unique ($R_{int}$ = 0.0528); giving $R_1$ = 0.0275, $wR_2$ = 0.0588 for 4932 data with [$I > 2\sigma(I)$] and $R_1$ = 0.0437, $wR_2$ = 0.0641 for all 6222 data. Residual electron density (e$^-$ Å$^{-3}$) max/min: 0.659/−0.357.

**X-ray Crystal Structure of [L$^1$Pd]$_2$.** Single crystals were obtained as red blocks from a concentrated *n*-pentane solution at −35 °C in the glovebox. Crystal and refinement data for [L$^1$Pd]$_2$: $C_{50}H_{76}P_4Pd_2$; $M_r$ = 1013.79; monoclinic; space group $P2/n$; $a$ = 19.7619(12) Å; $b$ = 13.7004(9) Å; $c$ = 19.9613(13) Å; $\alpha$ = 90°; $\beta$ = 112.3640(10)°; $\gamma$ = 90°; $V$ = 4997.9(6) Å$^3$; $Z$ = 4; $T$ = 120(2) K; $\lambda$ = 0.71073 Å; $\mu$ = 0.879 mm$^{-1}$; $d_{calc}$ = 1.347 g cm$^{-3}$; 62 041 reflections collected; 8823 unique ($R_{int}$ = 0.0957); giving $R_1$ = 0.0610, $wR_2$ = 0.1128 for 6320 data with [$I > 2\sigma(I)$] and $R_1$ = 0.0927, $wR_2$ = 0.1250 for all 8823 data. Residual electron density (e$^-$ Å$^{-3}$) max/min: 3.044/−2.222.

**X-ray Crystal Structure of L$^2$Pd.** Single crystals were obtained as gray blocks from a concentrated *n*-pentane at −35 °C in the glovebox. Crystal and refinement data for L$^2$Pd: $C_{26}H_{40}P_2Pd$; $M_r$ = 520.92; monoclinic; space group $P2(1)/c$; $a$ = 11.089(3) Å; $b$ = 14.971(4) Å; $c$ = 15.505(4) Å; $\alpha$ = 90°; $\beta$ = 102.693(4)°; $\gamma$ = 90°; $V$ = 2511.2(12) Å$^3$; $Z$ = 4; $T$ = 120(2) K; $\lambda$ = 0.71073 Å; $\mu$ = 0.877 mm$^{-1}$; $d_{calc}$ = 1.378 g cm$^{-3}$; 33 869 reflections collected; 4417 unique ($R_{int}$ = 0.0321); giving $R_1$ = 0.0212, $wR_2$ = 0.0563 for 4120 data with [$I > 2\sigma(I)$] and $R_1$ = 0.0235, $wR_2$ = 0.0575 for all 4417 data. Residual electron density (e$^-$ Å$^{-3}$) max/min: 0.379/−0.350.

**X-ray Crystal Structure of L$^2$Pd(*p*-C$_6$H$_4$−NO$_2$)Br.** Single crystals were obtained from a concentrated toluene solution layered with *n*-pentane at −35 °C in the glovebox. Crystal and refinement data for L$^2$Pd(*p*-C$_6$H$_4$−NO$_2$)Br: $C_{39}H_{52}BrNO_2P_2Pd$; $M_r$ = 815.07; triclinic; space group $P\bar{1}$; $a$ = 10.9023(4) Å; $b$ = 11.6680(4) Å; $c$ = 16.3181(6) Å; $\alpha$ = 80.5340(10)°; $\beta$ = 83.7490(10)°; $\gamma$ = 68.3020(10)°; $V$ = 1899.83(12) Å$^3$; $Z$ = 2; $T$ = 120(2) K; $\lambda$ = 0.71073 Å; $\mu$ = 1.658 mm$^{-1}$; $d_{calc}$ = 1.425 g cm$^{-3}$; 20 759 reflections collected; 6678 unique ($R_{int}$ = 0.0243); giving $R_1$ = 0.0261, $wR_2$ = 0.0630 for 5973 data with [$I > 2\sigma(I)$] and $R_1$ = 0.0312, $wR_2$ = 0.0651 for all 6678 data. Residual electron density (e$^-$ Å$^{-3}$) max/min: 0.793/−0.761.

**DFT Calculations.** DFT calculations were carried out using Gaussian03 (revision D.02). The B3LYP (DFT) method was used to carry out geometry optimizations on the model compounds specified in the text, using the LANL2DZ basis set. The validity of the true minima was checked by the absence of negative frequencies in the energy Hessian.

## ■ ASSOCIATED CONTENT

### Ⓢ Supporting Information

NMR spectra, crystallographic information (cif), and DFT calculation details. This material is available free of charge via the Internet at http://pubs.acs.org.

## ■ AUTHOR INFORMATION


### Corresponding Author

*E-mail: viluc@nd.edu.


### Notes

The authors declare no competing financial interest.

## ■ ACKNOWLEDGMENTS

We gratefully acknowledge discussions with Dr. Allen Oliver and funding from the University of Notre Dame (South Bend, IN, USA). The MS results are supported by the National Science Foundation (NSF) (under No. CHE-0741793).

## REFERENCES


(1) van Leeuwen, P. W. N. M.; Kamer, P. C. J.; Reek, J. N. H.; Dierkes, P. *Chem. Rev.* **2000**, *100*, 2741.
(2) Suseno, S.; Agapie, T. *Organometallics* **2013**, *32*, 3161.
(3) Birkholz, M.-N.; Freixa, Z.; van Leeuwen, P. W. N. M. *Chem. Soc. Rev.* **2009**, *38*, 1099.
(4) Xie, J.-H.; Zhou, Q.-L. *Acc. Chem. Res.* **2008**, *41*, 581.
(5) Shimizu, H.; Nagasaki, I.; Saito, T. *Tetrahedron* **2005**, *61*, 5405.
(6) Barbaro, P.; Bianchini, C.; Giambastiani, G.; Parisel, S. L. *Coord. Chem. Rev.* **2004**, *248*, 2131.
(7) Freixa, Z.; van Leeuwen, P. W. N. M. *Coord. Chem. Rev.* **2008**, *252*, 1755.
(8) Blakemore, J. D.; Chalkley, M. J.; Farnaby, J. H.; Guard, L. M.; Hazari, N.; Incarvito, C. D.; Luzik, E. D., Jr.; Suh, H. W. *Organometallics* **2011**, *30*, 1818.
(9) Wang, X.; Guo, P.; Han, Z.; Wang, X.; Wang, Z.; Ding, K. *J. Am. Chem. Soc.* **2013**, *136*, 405.
(10) Jarvis, A. G.; Sehnal, P. E.; Bajwa, S. E.; Whitwood, A. C.; Zhang, X.; Cheung, M. S.; Lin, Z.; Fairlamb, I. J. S. *Chem.—Eur. J.* **2013**, *19*, 6034.
(11) Wang, N.; McCormick, T. M.; Ko, S.-B.; Wang, S. *Eur. J. Inorg. Chem.* **2012**, 4463.
(12) Jacquet, O.; Clement, N. D.; Blanco, C.; Martinez Belmonte, M.; Benet-Buchholz, J.; van Leeuwen, P. W. N. M. *Eur. J. Org. Chem.* **2012**, 4844.
(13) Newman, P. D.; Cavell, K. J.; Kariuki, B. M. *Dalton Trans.* **2012**, *41*, 12395.
(14) Cai, F.; Pu, X.; Qi, X.; Lynch, V.; Radha, A.; Ready, J. M. *J. Am. Chem. Soc.* **2011**, *133*, 18066.
(15) Canac, Y.; Debono, N.; Lepetit, C.; Duhayon, C.; Chauvin, R. *Inorg. Chem.* **2011**, *50*, 10810.
(16) Koblenz, T. S.; Dekker, H. L.; de Koster, C. G.; van Leeuwen, P. W. N. M.; Reek, J. N. H. *Eur. J. Inorg. Chem.* **2011**, 4837.
(17) Ding, K.; Miller, D. L.; Young, V. G.; Lu, C. C. *Inorg. Chem.* **2011**, *50*, 2545.
(18) Schuecker, R.; Mereiter, K.; Spindler, F.; Weissensteiner, W. *Adv. Synth. Catal.* **2010**, *352*, 1063.
(19) Kaganovsky, L.; Gelman, D.; Rueck-Braun, K. *J. Organomet. Chem.* **2010**, *695*, 260.
(20) Nasser, N.; Eisler, D. J.; Puddephatt, R. J. *Chem. Commun.* **2010**, *46*, 1953.
(21) Lin, S.; Herbert, D. E.; Velian, A.; Day, M. W.; Agapie, T. *J. Am. Chem. Soc.* **2013**, *135*, 15830.
(22) Casey, C. P.; Whiteker, G. T.; Campana, C. F.; Powell, D. R. *Inorg. Chem.* **1990**, *29*, 3376.
(23) Destefano, N. J.; Johnson, D. K.; Lane, R. M.; Venanzi, L. M. *Helv. Chim. Acta* **1976**, *59*, 2674.
(24) Boronrettore, P.; Grove, D. M.; Venanzi, L. M. *Helv. Chim. Acta* **1984**, *67*, 65.
(25) Clapham, S. E.; Hadzovic, A.; Morris, R. H. *Coord. Chem. Rev.* **2004**, *248*, 2201.
(26) van der Vlugt, J. I.; Reek, J. N. H. *Angew. Chem., Int. Ed.* **2009**, *48*, 8832.
(27) Gunanathan, C.; Milstein, D. *Acc. Chem. Res.* **2011**, *44*, 588.
(28) Friedrich, A.; Drees, M.; Kass, M.; Herdtweck, E.; Schneider, S. *Inorg. Chem.* **2010**, *49*, 5482.
(29) He, T.; Tsvetkov, N. P.; Andino, J. G.; Gao, X. F.; Fullmer, B. C.; Caulton, K. G. *J. Am. Chem. Soc.* **2010**, *132*, 910.
(30) Grutzmacher, H. *Angew. Chem., Int. Ed.* **2008**, *47*, 1814.
(31) Khusnutdinova, J. R.; Rath, N. P.; Mirica, L. M. *J. Am. Chem. Soc.* **2010**, *132*, 7303.
(32) Annibale, V. T.; Song, D. *R. Soc. Chem. Adv.* **2013**, *3*, 11432.
(33) Weinberger, D. A.; Higgins, T. B.; Mirkin, C. A.; Stern, C. L.; Liable-Sands, L. M.; Rheingold, A. L. *J. Am. Chem. Soc.* **2001**, *123*, 2503.
(34) Slone, C. S.; Mirkin, C. A.; Yap, G. P. A.; Guzei, I. A.; Rheingold, A. L. *J. Am. Chem. Soc.* **1997**, *119*, 10743.
(35) Anderson, J. S.; Rittle, J.; Peters, J. C. *Nature* **2013**, *501*, 84.
(36) Zhang, W.-H.; Chien, S. W.; Hor, T. S. A. *Coord. Chem. Rev.* **2011**, *255*, 1991.
(37) van der Vlugt, J. I. *Eur. J. Inorg. Chem.* **2012**, 363.
(38) Barrett, B. J.; Iluc, V. M. *Organometallics* **2014**, *33*, 2565.
(39) Barrett, B. J.; Iluc, V. M. *Inorg. Chem.* **2014**, *53*, 7248.
(40) Burford, R. J.; Piers, W. E.; Ess, D. H.; Parvez, M. *J. Am. Chem. Soc.* **2014**, *136*, 3256.
(41) Gutsulyak, D. V.; Piers, W. E.; Borau-Garcia, J.; Parvez, M. *J. Am. Chem. Soc.* **2013**, *135*, 11776.
(42) Burford, R. J.; Piers, W. E.; Parvez, M. *Eur. J. Inorg. Chem.* **2013**, *2013*, 3826.
(43) Burford, R. J.; Piers, W. E.; Parvez, M. *Organometallics* **2012**, *31*, 2949.
(44) Lesueur, W.; Solari, E.; Floriani, C.; Chiesi-Villa, A.; Rizzoli, C. *Inorg. Chem.* **1997**, *36*, 3354.
(45) Hofer, A.; Kovacs, G.; Zappatini, A.; Leuenberger, M.; Hediger, M. A.; Lochner, M. *Bioorg. Med. Chem.* **2013**, *21*, 3202.
(46) Wyatt, P.; Hudson, A.; Charmant, J.; Orpen, A. G.; Phetmung, H. *Org. Biomol. Chem.* **2006**, *4*, 2218.
(47) Tang, W.; Capacci, A. G.; White, A.; Ma, S.; Rodriguez, S.; Qu, B.; Savoie, J.; Patel, N. D.; Wei, X.; Haddad, N.; Grinberg, N.; Yee, N. K.; Krishnamurthy, D.; Senanayake, C. H. *Org. Lett.* **2010**, *12*, 1104.
(48) Brookhart, M.; Green, M. L. H.; Parkin, G. *Proc. Natl. Acad. Sci. U.S.A.* **2007**, *104*, 6908.
(49) Sundquist, W. I.; Bancroft, D. P.; Lippard, S. J. *J. Am. Chem. Soc.* **1990**, *112*, 1590.
(50) Braga, D.; Grepioni, F.; Tedesco, E.; Biradha, K.; Desiraju, G. R. *Organometallics* **1997**, *16*, 1846.
(51) Zhang, Y.; Lewis, J. C.; Bergman, R. G.; Ellman, J. A.; Oldfield, E. *Organometallics* **2006**, *25*, 3515.
(52) Braga, D.; Grepioni, F.; Biradha, K.; Desiraju, G. R. *J. Chem. Soc.-Dalton Trans.* **1996**, 3925.
(53) Mukhopadhyay, A.; Pal, S. *Eur. J. Inorg. Chem.* **2006**, 4879.
(54) Slough, G. A.; Bergman, R. G.; Heathcock, C. H. *J. Am. Chem. Soc.* **1989**, *111*, 938.
(55) Yin; Liebscher, J. *Chem. Rev.* **2006**, *107*, 133.
(56) Jimenez-Rodriguez, C.; Roca, F. X.; Bo, C.; Benet-Buchholz, J.; Escudero-Adan, E. C.; Freixa, Z.; van Leeuwen, P. W. N. M. *Dalton Trans.* **2006**, 268.
(57) Deraedt, C.; Astruc, D. *Acc. Chem. Res.* **2014**, *47*, 494.
(58) de Vries, A. H. M.; Mulders, J.; Mommers, J. H. M.; Henderickx, H. J. W.; de Vries, J. G. *Org. Lett.* **2003**, *5*, 3285.
(59) de Vries, J. G. *Dalton Trans.* **2006**, 421.
(60) Alonso, F.; Beletskaya, I. P.; Yus, M. *Tetrahedron* **2005**, *61*, 11771.
(61) Beletskaya, I. P.; Cheprakov, A. V. *J. Organomet. Chem.* **2004**, *689*, 4055.
(62) Phan, N. T. S.; Van Der Sluys, M.; Jones, C. W. *Adv. Synth. Catal.* **2006**, *348*, 609.
(63) Reetz, M. T.; de Vries, J. G. *Chem. Commun.* **2004**, 1559.
(64) Biffis, A.; Zecca, M.; Basato, M. *J. Mol. Catal. A: Chem.* **2001**, *173*, 249.
(65) Grushin, V. V.; Marshall, W. J. *J. Am. Chem. Soc.* **2006**, *128*, 12644.
(66) Yin, J.; Buchwald, S. L. *J. Am. Chem. Soc.* **2002**, *124*, 6043.
(67) Zuideveld, M. A.; Swennenhuis, B. H. G.; Boele, M. D. K.; Guari, Y.; van Strijdonck, G. P. F.; Reek, J. N. H.; Kamer, P. C. J.; Goubitz, K.; Fraanje, J.; Lutz, M.; Spek, A. L.; van Leeuwen, P. W. N. M. *J. Chem. Soc., Dalton Trans.* **2002**, 2308.
(68) Czauderna, C.; Wurziger, H.; Sun, Y.; Thiel, W. R. *Z. Anorg. Allg. Chem.* **2008**, *634*, 2380.
(69) Morgan, B. P.; Galdamez, G. A.; Gilliard, R. J.; Smith, R. C. *Dalton Trans.* **2009**, 2020.
(70) Diederich, F.; Stang, P. J. *Metal Catalyzed Cross-Coupling Reactions*; Wiley−VCH: New York, 1998.